Production delays and price dynamics

Hommes, C.; Li, K.; Wagener, F.

DOI
10.1016/j.jebo.2021.12.033
Publication date
2022
Document Version
Final published version
Published in
Journal of Economic Behavior and Organization

Journal of Economic Behavior and Organization 194 (2022) 341–362

Contents lists available at ScienceDirect

Journal of Economic Behavior and Organization

journal homepage: www.elsevier.com/locate/jebo

Production delays and price dynamics

Cars Hommes[a,b], Kai Li[c,d,*], Florian Wagener[a]

[a] CeNDEF, Amsterdam School of Economics University of Amsterdam, 1001 NJ Amsterdam, The Netherlands
[b] Bank of Canada, Ottawa, Canada
[c] Macquarie Business School Macquarie University, NSW 2109, Australia
[d] Institute of Financial Studies Southwestern University of Finance and Economics, Chengdu, China

ARTICLE INFO

Article history:
Received 10 February 2021
Revised 21 December 2021
Accepted 27 December 2021
Available online 5 January 2022

JEL classification:
C62
D84
E32

Keywords:
Cobweb model
Heterogeneity
Adaptiveness
Production delay
Stability
Chaos

ABSTRACT

This paper develops a unified analysis of the impacts of production delays on aggregate price fluctuations in a continuous-time cobweb-type model. We find that the time inconsistency between demand and supply due to production delays inherently generates an overshooting effect in prices. Large production delays give rise to price fluctuations, even with a low intensity of choice. We also provide results consistent with the *rational route to randomness* of Brock and Hommes (1997) in a continuous-time infinite-dimensional economy.

1. Introduction

Cobweb theory describes a dynamic price adjustment process for a good with a supply response lag. The key message conveyed by the theory is that price fluctuations can be caused by the time delay needed to produce the good (we term this the production delay). Most cobweb models, developed on discrete-time scales, assume that it takes one unit of time to produce the good, and hence, the impact of the length of the production delay has seldom been studied. In this paper, we propose a unified cobweb-type price prediction system with adaptively heterogeneous beliefs in continuous time to systematically examine the impacts of both production delays and the belief distributions of agents on aggregate price fluctuations.

Our paper extends the discrete-time cobweb model in Brock and Hommes (1997) to a general continuous-time setting where producers form expectations about future prices by choosing price predictors based on their past performance and a market maker adjusts the price based on the current excess demand. In our continuous-time cobweb-type model, the production delay is simply presented by a parameter that allows a unified analysis of both production delays and producers' belief distributions. The predictor set can be infinite, and the resultant economy is infinite dimensional. This continuous-

* Corresponding author at: Macquarie Business School Macquarie University, NSW 2109, Australia.
E-mail addresses: C.H.Hommes@uva.nl (C. Hommes), kai.li@mq.edu.au (K. Li), F.O.O.Wagener@uva.nl (F. Wagener).

https://doi.org/10.1016/j.jebo.2021.12.033
0167-2681/

time framework with infinite beliefs is more realistic since production delays are not necessarily integers in reality and goods are traded in practice in continuous time.

We show that production delays inherently generate an overshooting effect, which can further destabilize the market. If there is no production delay, decisions of demand and supply are made at the same time. As a result, the economy is self-regulating in the sense that future price dynamics are completely determined by the current price. In this case, the system is globally stable, and the price converges to its steady-state level *monotonically*. With production delays, an overshooting effect occurs, which further leads to price oscillations. To elaborate, we consider that the initial price starts below its steady state. With a production delay, initial demand, which is based on the current price, is greater than initial supply, which is based on delayed prices, implying that the price will increase in following periods. However, when the price increases beyond its steady-state level, demand is still greater than supply due to the increasing price trend (or positive momentum); thus, the price keeps increasing even if it is already greater than its steady-state level. As a result, the *time inconsistency* between demand and supply decisions generates an overshooting in price dynamics, followed by interchanges between periods of demand being greater than supply and periods of demand being less than supply. If the production delay is short, the time inconsistency is small. In this case, agents can easily adjust their demand and supply accordingly, and the system can eventually digest the time inconsistency, leading to *consistency* between demand and supply and hence a stable price in the long run. However, a significant production delay leads to a large time inconsistency that cannot be absorbed by the system. As a result, the overshooting effect leads to constant, long-lasting price fluctuations.

This overshooting effect is inherent to production delays. Without a delay, the system is linear; hence, the price monotonically converges to the steady-state level without overshooting. With a delay, the system becomes nonlinear, and price overshooting occurs regardless of whether the system is stable. However, changes in other parameters cannot change the overshooting effect since they do not alter the nonlinearity of the system, highlighting the important and distinctive role of production delays. We observe large price fluctuations even for a low intensity of choice as long as the production delay is large—a topic on which there is little research in the discrete-time cobweb literature.

Our model also verifies the *rational route to randomness* of Brock and Hommes (1997). In addition to production delays, population evolution is another economic channel through which the market is destabilized. When the perfect-foresight predictor is subject to positive information costs, producers switch between perfect-foresight and naive predictors, and a high intensity of choice leads to price fluctuations and even chaos. We show that as the intensity of choice increases, the fixed point dynamics turn via a sequence of bifurcations into chaotic dynamics. To the best of our knowledge, our paper provides the first numerical example of chaotic dynamics in *an infinite-dimensional economy*. Chaos has been found in discrete-time nonlinear cobweb models due to either a highly nonlinear supply curve (e.g., Jensen and Urban, 1984) or adaptive behavior (e.g., Chiarella, 1988; Brock and Hommes, 1997). Motivated by the evidence from laboratory experiments (e.g., Hommes et al., 2007 and Hommes, 2011), we assume that producers adaptively update their beliefs. The adaptive behavior in our model generates chaos even with linear demand and supply curves. Chaotic price dynamics have also been documented in strategy experiments in a cobweb framework, as in, e.g., Sonnemans et al. (2004).

Indeed, with a high intensity of choice, the unique steady state is a saddle point. For an initial state with most producers using naive predictors, the price cyclically departs from the steady-state price since the initial state lies in the unstable manifold of the steady state. As long as the deviation of the price from its steady-state level is large enough that the perfect-foresight predictor has a higher net profit than naive predictors, (almost) all producers immediately switch to the perfect-foresight predictor, and the price suddenly converges to its steady state. After this, once the orbit lies in the stable manifold of the steady state, the system converges to the saddle-point steady state. As a result, we observe that the price builds up slowly but crashes suddenly, and that, in the meanwhile, market fractions move slowly but experience sudden jumps. In this case, adding a small amount of noise to the system would lead to very irregular price fluctuations.

Most cobweb models study only one type of naive predictor. The use of more predictors by producers gives rise to higher-dimensional systems, which are rather difficult to analyze.[1] Our continuous-time model with (distributed) time delays inherently contains an infinite number of predictors and hence facilitates the analysis of belief distributions among producers. On the one hand, by examining some examples of exogenous distributions, we find that the belief distributions can significantly affect market stability. Unlike the discrete-time model in Brock and Hommes (1997), our economy tends to be stable with uniformly distributed beliefs.[2] On the other hand, when producers update their beliefs based on certain fitness measures, different price dynamics can, in turn, lead to different belief distributions. The belief distribution is "stationary" when the price is stable with a low intensity of choice, while it becomes "nonstationary" and fluctuates widely when the price is unstable.

The classical linear cobweb model of Ezekiel (1938), in which homogeneous producers simply use naive predictors, provides an explanation of the cyclical price behavior observed in many commodity markets. However, linear demand and supply make the models unable to generate stable oscillations. Prompted by the growing popularity of applications of nonlinear dynamics theory in finance and economics, cobweb models have been extended in two directions over the last three decades. By exploring nonlinearities in the supply and demand curves, Jensen and Urban (1984) and Hommes

[1] Branch (2002), Onozaki et al. (2003) and Diks and van der Weide (2005) are a few exceptions who consider more than one type of naive predictors.

[2] In fact, the infinite predictor set in the continuous-time setup includes almost-perfect-foresight predictors. The price movements become predictable under these predictors, and countercyclical production responses can smooth out market fluctuations, causing the cycle to disappear.

(1998, 2018) analytically show that cobweb models exhibit stable periodic and complex price dynamics. On the other hand, Brock and Hommes (1997) develops a cobweb model in which heterogeneous producers choose predictors from a large set of predictor functions of past prices and update their beliefs over time according to a fitness measure. They show that the equilibrium dynamics are coupled with the population evolutions, exhibiting the rational route to randomness. This framework has been extended to consider different learning schemes (Chiarella and He, 2003) and multiple goods markets (Dieci and Westerhoff, 2010). Our continuous-time model contributes to the development of the cobweb literature in both directions by providing a unified treatment of different time delays used to form predictors in discrete-time cobweb models.

In discrete-time models, different delays lead to very different systems of different dimensions that need to be analyzed separately; in particular, when the time horizon for historical information is long, the resultant discrete-time models are high-dimensional systems, which are difficult to analyze (Chiarella and He, 2003). The continuous-time setup developed in this paper overcomes this limitation. Our model is characterized mathematically by a system of delay differential equations (DDEs), and the production delay is simply characterized by a parameter, allowing a unified analysis of the delay effect.[3]

The paper is organized as follows. In Section 2, we develop a continuous-time cobweb-type model with heterogeneous beliefs to explicitly characterize the production delay effect. In Section 3, we apply stability and bifurcation theory to examine the impacts of production delays and population evolution. Section 4 concludes. All the proofs and model extensions are included in the appendices.

2. The model

In this section, we develop a continuous-time cobweb-type model with heterogeneous beliefs and adaptive behavior to explicitly characterize the time-delay effect. The good price is jointly determined by aggregate demand and supply. Let $D(\cdot)$ and $S(\cdot)$ be the demand and supply functions at time t, respectively. Assume that consumer demand $D(P_t)$ depends upon the current market price P_t and is strictly decreasing in price.

There is a continuum of producers who can be grouped into N types. As "*wine is not made in a day*," as emphasized by Kydland and Prescott (1982), we assume that it takes $\tau \geq 0$ units of time to produce the good for all producers. Parameter τ represents the time to produce (or the production delay). This implies that production decisions about the amount of output to be delivered at time t are made at time $t-\tau$. To make production decisions, producers need to predict the future price at time t. Each producer can choose her predictor from a predictor set. Assume that the predictor of type-i producers, namely, $H^i_{t-\tau} = H^i(P_u : u \leq t)$, depends on prices prior to time t. In particular, type-i producers have perfect foresight when $H^i_{t-\tau} = P_t$; however, some producers may predict the future price based only on the current price $H^i_{t-\tau} = P_{t-\tau}$, which we term a naive predictor.

The supply curve $S(H^i_{t-\tau})$ is derived from firms maximizing profits with a cost function $c(q)$, where q is the supply of the good. That is,

$$S(H^i_{t-\tau}) = \text{argmax}\left\{H^i_{t-\tau} q_{t-\tau} - c(q_{t-\tau})\right\} = (c')^{-1}(H^i_{t-\tau}), \tag{2.1}$$

which is assumed to be increasing in the expected price. Let n^i_t be the market fraction of type-i producers at time t. Then, the total supply at time t is given by $\sum_{i=1}^N n^i_{t-\tau} S(H^i_{t-\tau})$. Note that because of the production delay, the supply delivered at time t is determined by the market fractions $n^i_{t-\tau}$ at time $t-\tau$.

We model the evolution of the market fraction of type-i producers, n^i_t, using discrete choice models (Anderson et al., 1992), which have been widely used in the heterogeneous agent models literature to characterize adaptive behavior. That is,

$$n^i_t = \frac{e^{\beta U^i_t}}{\sum_{j=1}^N e^{\beta U^j_t}}, \qquad i = 1, 2, \cdots, N, \tag{2.2}$$

where U^i is the performance measure to be specified below and the parameter $\beta \geq 0$ is the intensity of choice, measuring how fast producers switch predictors. In particular, there is no switching among producers if $\beta = 0$, while all producers immediately switch to the optimal predictor if $\beta = \infty$.

Following Brock and Hommes (1997, 1998), we assume that the predictor is chosen based upon its past performance. The realized net profit π^i from using predictor $H^i_{t-\tau}$ at time t is given by

$$\pi^i_t = P_t S(H^i_{t-\tau}) - c\big(S(H^i_{t-\tau})\big) - C^i, \tag{2.3}$$

where $c(\cdot)$ is the producer's cost function and $C^i \geq 0$ is constant information cost for obtaining predictor H^i. The performance U^i_t of predictor H^i at time t is a weighted average of past realized net profits measured by

$$U^i_t = \eta \int_{-\infty}^t e^{-\eta(t-s)} \pi^i_s ds, \tag{2.4}$$

[3] Applications of delay differential equations to characterize cyclical economic behavior have a long history; see, e.g., Haldane (1932) and Mackey (1989). This development has further led to studies on the effect of policy lags on macroeconomic stability in Phillips (1957), Asada and Yoshida (2001), and Yoshida and Asada (2007), asset pricing models in Di Guilmi et al. (2014) and Guo et al. (2020), and portfolio management in Li and Liu (2018, 2021) and Li (2019).

where the decay parameter $\eta > 0$ represents the "memory strength". As η increases, the weights on the latest realized profits increase. In particular, $U_t^i = \pi_t^i$ when $\eta \to \infty$. We will show in Section 3.3.3 that the memory strength η governs the relative speed of price dynamics and population evolution. It follows from (2.4) that

$$\dot{U}_t^i = \eta(\pi_t^i - U_t^i). \tag{2.5}$$

Therefore, the population evolution is characterized by (2.2)–(2.5).[4]

As in most heterogenous agent models in which agents are allowed to switch among predictors, the discrete choice model (2.2) assumes that the firms are boundedly rational and make their decisions according to certain heuristic statistics. More specifically, the firms do not have perfect knowledge about the accuracy of the predictors. They evaluate the predictors based only on their past performance as measured by (2.3)–(2.4), and each time period they use one predictor chosen from the N-predictor set. As a result, the firms do not base their choice of predictors on other factors, such as price persistence or reusage of recent costly information.[5]

The producers sell their product not on an open market but to a retail firm. This firm posts daily prices and buys all output at that price. It adjusts the prices based on excess demand (e.g., Mackey, 1989):[6]

$$\dot{P}_t = \alpha\left[D(P_t) - \sum_{i=1}^{N} n_{t-\tau}^i S(H_{t-\tau}^i)\right], \tag{2.6}$$

where $\alpha > 0$ is the price adjustment coefficient. The price adjustment rule (2.6) is similar to the market-maker scenario widely studied in the context of financial markets, e.g., Beja and Goldman (1980) and Day and Huang (1990). To focus on production delays, we do not model the retailer's storage or the inventory of a "market maker". We refer readers to Mitra and Boussard (2012) for the effect of storage on price dynamics in a nonlinear cobweb model and Franke and Asada (2008) and Zhu et al. (2009) for the effect of market inventories.

To complete the model, we need to specify the demand and supply functions. In this paper, we base our main analysis on linear demand and supply curves, that is,

$$\begin{aligned} D(P_t) &= A - dP_t, \qquad A > 0, \qquad d > 0, \\ S(H_{t-\tau}^i) &= sH_{t-\tau}^i, \qquad s > 0, \end{aligned}$$

where the supply curve is derived from a quadratic cost function $c(q_t) = q_t^2/2s$. We discuss nonlinear demand and supply in Appendix C. We find that the main findings in the linear case still hold with nonlinear supply curves, although nonlinear supply generates more involved comovements between price and population.

In all, the price is determined by the following cobweb-type predictive system with adaptively heterogeneous beliefs in continuous time:

$$\begin{cases} \dot{P}_t &= \alpha\left[D(P_t) - \sum_{i=1}^{N} n_{t-\tau}^i S(H_{t-\tau}^i)\right], \\ \dot{U}_t^i &= \eta(\pi_t^i - U_t^i), \quad i = 1, \cdots, N, \end{cases} \tag{2.7}$$

where n_t^i is governed by (2.2) and π_t^i is given by (2.3). System (2.7) is a nonlinear differential system with time delays and $N + 1$ state variables.

3. The impacts of production delays and population evolution

In this section, we study the impacts of both production delays and population evolution on the price dynamics. We start with two special cases to provide a first glance at the roles of different predictors and production delays in Sections 3.1–3.2. We then examine the interaction of production delays and population evolution by considering two types of beliefs used by the producers in Section 3.3. A general model with an infinite number of beliefs is studied in Section 3.4 to examine the impact of belief distributions.

3.1. Perfect-foresight predictor

We first discuss a special case in which all producers use a perfect-foresight predictor:[7]

$$H_{t-\tau} = P_t,$$

[4] He and Li (2012) show that the above discrete choice model (2.2)–(2.5) in continuous time is consistent with replicator dynamics (Hofbauer and Sigmund, 1998).

[5] The non-reusage of recently purchased information can be also consistent with an economy in which in different time periods different sets of firms enter the market, like overlapping generations, and choose their predictors without sharing information across firms.

[6] The alternative assumption, that the *relative* variation in market price $\dot{P}/P$ is proportional to excess demand, leads to a more unstable steady state $P^* = 0$, which we are not interested in. In this paper, we consider that the impact of excess demand is at the price level in (2.6).

[7] This case is equivalent to the case without a production delay.

that is, the producers have perfect knowledge of the future price. In this case, the supply curve satisfies $S(H_{t-\tau}) = sP_t$, and (2.7) reduces to

$$\dot{P}_t = \alpha\big(A - dP_t - sP_t\big). \tag{3.1}$$

Brock and Hommes (1997) show that the equilibrium price is stable in discrete time. The following proposition confirms the stabilizing role of the perfect-foresight predictor in continuous time.

Proposition 3.1. *System (3.1) has a unique steady-state price $P^* = A/(d+s)$, which is globally stable.*

Appendix A.1 contains the proof for this proposition.[8] Proposition 3.1 shows that when there is no time delay, the steady state is globally stable. The price with any initial values converges monotonically and quickly to the steady state. We provide further discussions about the adjustment path in Section 3.3.2.

3.2. Naive predictors

To examine the time-delay effect, we study another special case in which all agents use the same naive predictor,

$$H_{t-\tau} = P_{t-\tau}. \tag{3.2}$$

That is, they predict the future price and make production decisions based on only the current price. Note that predictor (3.2) coincides with the perfect-foresight predictor when $\tau = 0$. The price dynamics are given by

$$\dot{P}_t = \alpha\big(A - dP_t - sP_{t-\tau}\big). \tag{3.3}$$

Classical discrete-time cobweb models suggest that naive predictors based on past prices may destabilize the market, and the following proposition verifies this.

Proposition 3.2.

(1) *System (3.3) has a unique steady-state price $P^* = A/(d+s)$.*
(2) *If $s \le d$, then P^* is locally asymptotically stable for all $\tau \ge 0$.*
(3) *If $s > d$, then P^* is locally asymptotically stable for $0 \le \tau < \tau_0^{**}$ and unstable for $\tau > \tau_0^{**}$.*

Proposition 3.2 shows that when $s/d < 1$, the steady-state price is stable for any production delay. If the relative supply strength is, however, high, the steady-state price is stable only for small production delays, and it is destabilized if the delay grows sufficiently large. Interestingly, unlike discrete-time models, Proposition 3.2 states that a small time delay can play stabilizing role. Intuitively, when the time delay is small enough, the predictor is very close to achieving perfect foresight, and hence, the system is stable. The destabilizing role of a large production delay is also found in Mackey (1989), Gori et al. (2014, 2015), Matsumoto and Nakajama (2015), and Matsumoto and Szidarovszky (2015). In addition, d plays a stabilizing role, while s and α play destabilizing roles in the market, in the sense that an increase in d increases τ_0^{**} and hence tends to stabilize the market while an increase in s or α decreases τ_0^{**} and hence destabilizes the market, as shown in Appendix A.2.[9]

3.3. Adaptive behavior with perfect-foresight and naive predictors

This section studies the joint impact of heterogeneous beliefs and adaptive behavior. For simplicity, we consider only two predictor types: perfect-foresight and naive predictors: that is,

$$H^R_{t-\tau} = P_t \quad \text{and} \quad H^N_{t-\tau} = P_{t-\tau}.$$

Naive predictors are assumed to be freely available, whereas perfect-foresight predictors can be obtained at an information cost $C^R \ge 0$. In accordance with (2.3), realized net profits are then given by

$$\pi^R_t = P_t S^R_t - c(S^R_t) - C_R = sP_t^2 - \frac{s}{2}P_t^2 - C_R = \frac{s}{2}P_t^2 - C_R, \tag{3.4}$$

$$\pi^N_t = P_t S^N_t - c(S^N_t) = sP_tP_{t-\tau} - \frac{s}{2}P^2_{t-\tau} = \frac{s}{2}P_{t-\tau}(2P_t - P_{t-\tau}). \tag{3.5}$$

This leads to the model:

$$\begin{cases} \dot{P}_t = \alpha\Big[A - dP_t - sn^R_{t-\tau}P_t - s(1-n^R_{t-\tau})P_{t-\tau}\Big], \\ \dot{U}^R_t = \eta\Big(\frac{s}{2}P_t^2 - C^R - U^R_t\Big), \\ \dot{U}^N_t = \eta\Big[\frac{s}{2}P_{t-\tau}(2P_t - P_{t-\tau}) - U^N_t\Big], \end{cases} \tag{3.6}$$

[8] In this paper, all proofs are included in the appendix.

[9] Technically speaking, the steady state does not undergo a Hopf bifurcation at $\tau = \tau_0^{**}$ since the genericity condition for Hopf bifurcation is not satisfied in the linear system (3.3).

where the market fraction of perfect-foresight agents n_t^R is given by

$$n_t^R = \frac{e^{\beta U_t^R}}{e^{\beta U_t^R} + e^{\beta U_t^N}} = \frac{1}{1 + e^{\beta (U_t^N - U_t^R)}}. \tag{3.7}$$

This states that the market fraction of perfect-foresight agents increases in the performance difference $U^R - U^N$.

3.3.1. The destabilizing effect of a large production delay

The price dynamics of (3.6) with respect to τ is described by the following proposition.

Proposition 3.3.

(1) *System (3.6) has a unique steady state* $(P^*, U^{R*}, U^{N*}) = (\frac{A}{d+s}, \frac{sA^2}{2(d+s)^2} - C^R, \frac{sA^2}{2(d+s)^2})$.
(2) *If* $s \le d/(1-2n^{R*})$, *then* (P^*, U^{R*}, U^{N*}) *is locally asymptotically stable for all* $\tau \ge 0$.
(3) *If* $s > d/(1-2n^{R*})$, *then* (P^*, U^{R*}, U^{N*}) *is locally asymptotically stable for* $0 < \tau < \tau_0^*$, *is unstable for* $\tau > \tau_0^*$, *and undergoes a Hopf bifurcation at* $\tau = \tau_0^*$, *where the Hopf bifurcation value* τ_0^* *is governed by (A.8).*

Proposition 3.3 shows that system (3.6) has the same steady-state price P^*, which is yielded in the homogeneous belief cases since both predictors deliver identical forecasts in the fundamental steady state. The steady-state fitness for the perfect-foresight predictor U^{R*} is its realized profit in the steady state less the cost C^R. The steady-state fitness of the naive predictor U^{N*} is its realized profit in the steady state, which is the same as that of the perfect-foresight predictor due to the fact that they share the same steady-state price. The market fraction of perfect-foresight agents in the steady state is $n^{R*} = (e^{\beta C^R} + 1)^{-1} \le 0.5$.

Consistent with Propositions 3.1–3.2, Proposition 3.3 again shows the stabilizing role of the perfect-foresight predictor and the destabilizing role of naive predictors even in the presence of population evolution. When $s \le d/(1-2n^{R*})$, the steady state is always stable, and the time delay τ and switching intensity β do not qualitatively affect the local stability of the market. When $s > d/(1-2n^{R*})$, the steady state is stable for a small time delay but becomes unstable for a large time delay. This is consistent with the results shown in Chiarella and He (2003), who examine several cases with short delays and find that price dynamics become more complex as the delay increases. Proposition 3.3 provides a systematic analysis on the delay effect. Note that the condition $s \le d/(1-2n^{R*})$ is weaker than the one in Proposition 3.2 and that Proposition 3.3 has a relatively larger stable interval with respect to the time delay than that in Proposition 3.2 ($\tau_0^* > \tau_0^{**}$). Thus, the adaptive system (3.6) with a population evolution between perfect-foresight and naive predictors is more stable than system (3.3), in which the market is full of naive traders. Intuitively, the total supply in (3.6) is a weighted average of perfect-foresight and naive expectations. The destabilizing role of naive expectations is partially offset by perfect-foresight expectations; hence, the system is more stable.

Furthermore, system (3.6) can be stabilized by increasing the parameter d or decreasing the parameters s, α, τ, β, and C^R (Appendix A.3). Especially when $\beta = 0$ or $C^R = 0$, the steady-state market fraction $n^{R*} = 0.5$, and the condition $s \le d/(1-2n^{R*})$ always holds, implying that the system is always stable. This result further highlights the importance of decreasing information costs and is consistent with Schmitt and Westerhoff (2015), who show that policy-makers can reduce the (steady-state) disadvantage of the stabilizing perfect-foresight predictor by imposing profit taxes, thereby managing (reversing) the model's rational route to randomness.

Interestingly, Proposition 3.3 shows that the decay parameter η does not affect *local* stability. However, it is in the higher-order terms of the system and hence can affect the *global* dynamics via the population-evolution process (He and Li, 2012).

Figure 3.1 illustrates the bifurcation diagram of prices with respect to τ for the case $s \le d/(1-2n^{R*})$. It confirms that the system is stable at small τ but becomes unstable at large τ. The left panel of Fig. 3.2 illustrates the time series of the fitness functions U^R and U^N when τ is chosen in the unstable region ($\tau = 10$), and the middle panel illustrates the market fraction of perfect-foresight traders and the price. Both panels show the periodic fluctuations in the price, associated with the fluctuations of the fitness functions of both perfect-foresight and naive expectations and hence their market fractions. The market fraction of perfect-foresight traders n^R increases with the fitness difference $U^R - U^N$. The phase plot in the right panel illustrates the opposite movements between the price and the market fraction of perfect-foresight traders, implying a stabilizing role of these traders.

Figure 3.2 illustrates the comovements of the price and market fractions. When the price increases to the steady-state value, associated with increases in the fraction of agents who choose the naive predictor, the price keeps increasing due to an overshooting effect, which is discussed shortly. The prices then diverge from the steady state, which leads to an increase in the prediction error from the naive predictor (or a decrease in the net profits of the naive predictor). When the net profit associated with the naive predictor becomes lower than that associated with the perfect-foresight predictor, agents are willing to pay some information cost to obtain the perfect-foresight predictor. Prices are then pushed back toward their steady-state level. With prices close to their steady-state value, the prediction error of the naive predictor becomes small again, and agents then switch their beliefs to the naive expectation without cost. As a result, agents switch between perfect-foresight and naive predictors over time, leading to price fluctuations. This observation verifies the adaptive rational equilibrium dynamics proposed in Brock and Hommes (1997), who observe this phenomenon with the premise of a high intensity of choice. However, for a given level of intensity of choice, our economy can always produce such price dynamics as long as there is a large production delay.

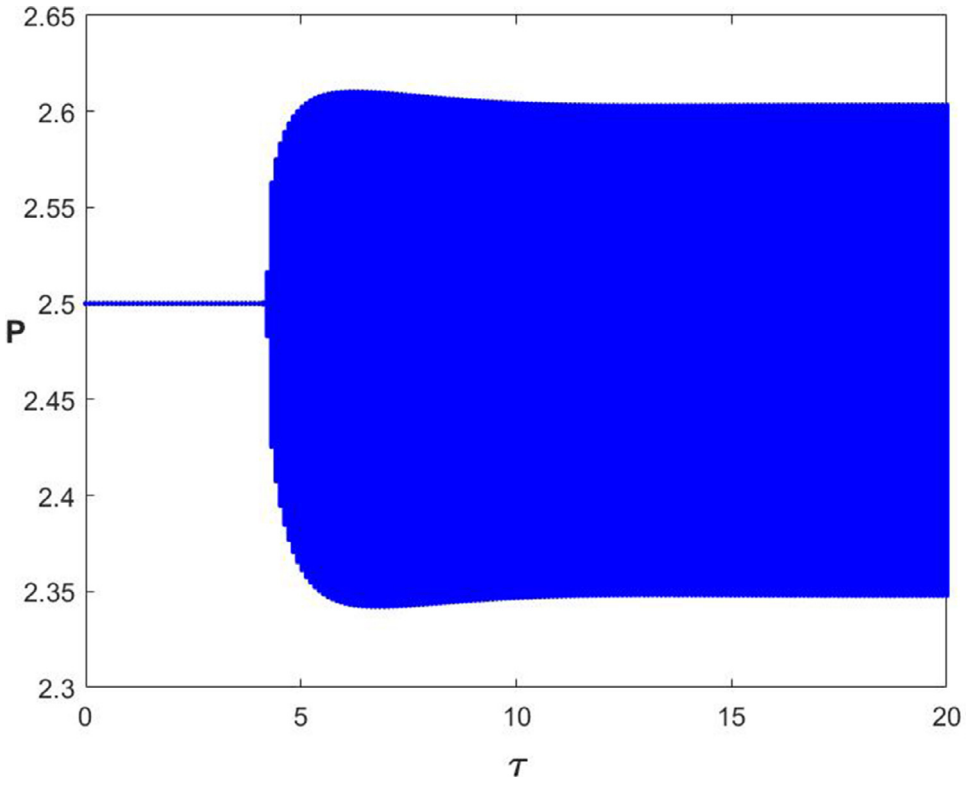

Fig. 3.1. The bifurcation diagram of the price with respect to τ. Here, $\beta = 1.3$, $\alpha = 1$, $A = 10$, $d = 1$, $s = 3$, $\eta = 0.5$, and $C^R = 0.6$. The steady state is $(P^*, U^{R*}, U^{N*}) = (2.5, 8.8, 9.4)$, and the market fraction of perfect-foresight traders in the steady state is $n^{R*} = 0.31$. This parameter set corresponds to the case $b > d/(1 - 2n^{R*})$.

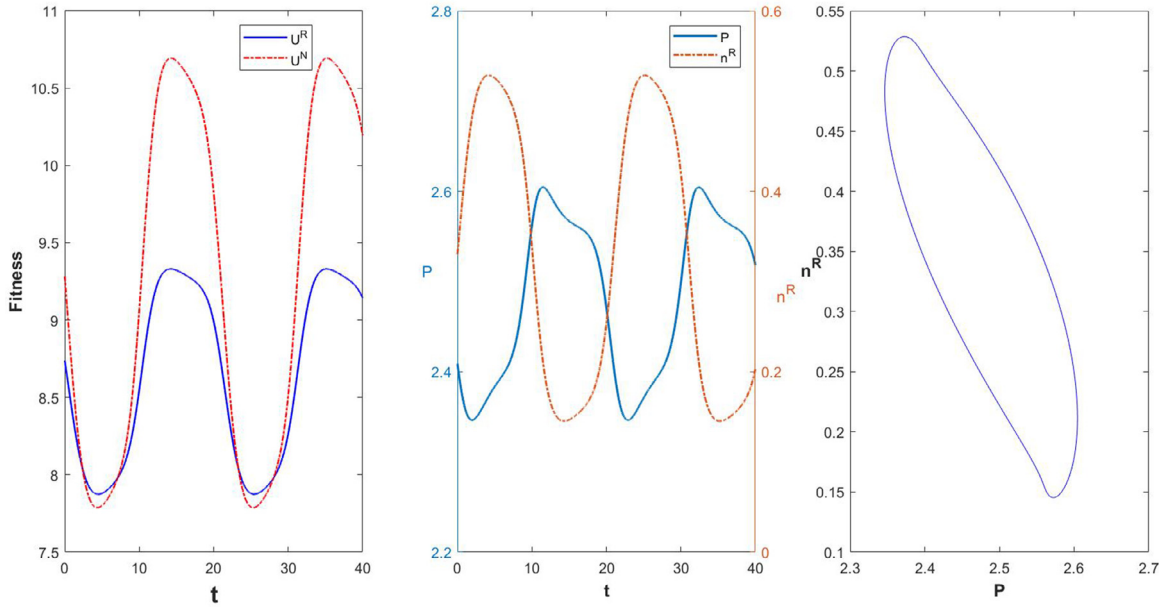

Fig. 3.2. The time series of the fitness functions of perfect-foresight and naive predictors (left panel) and of the price and market fraction of perfect-foresight traders (middle panel) and the phase plot (right panel). Here, $\beta = 1.3$, $\tau = 10$, $\alpha = 1$, $A = 10$, $d = 1$, $s = 3$, $\eta = 0.5$, and $C^R = 0.6$.

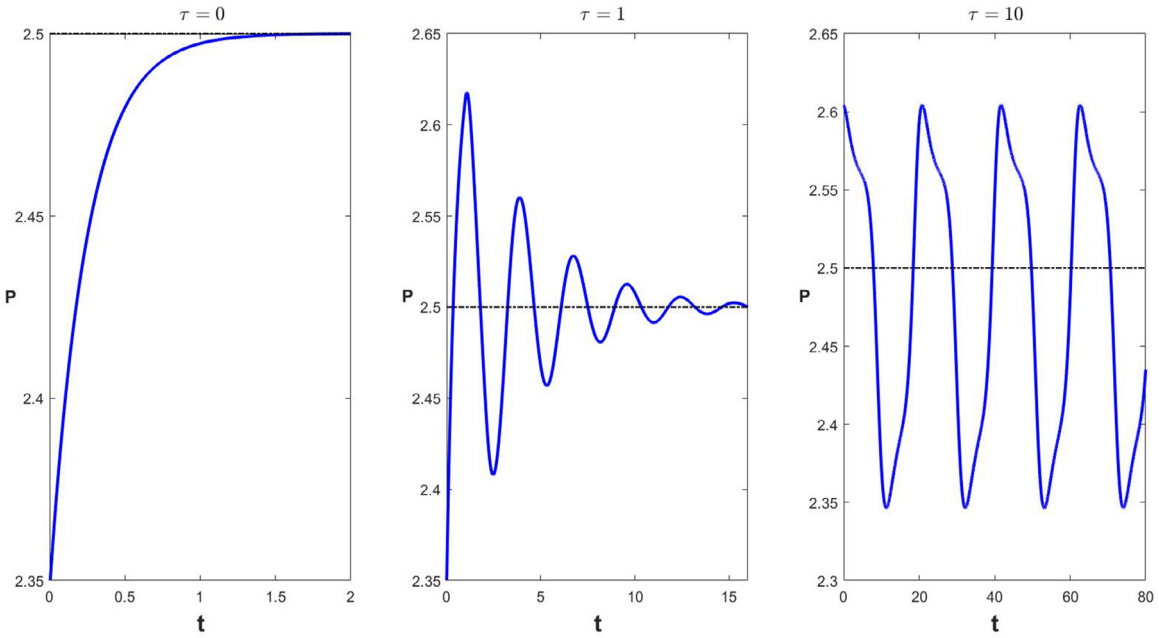

Fig. 3.3. Time series of price for $\tau = 0$ (left panel), $\tau = 1$ (middle panel), and $\tau = 10$ (right panel). Here, $\beta = 1.3$, $\alpha = 1$, $A = 10$, $d = 1$, $s = 3$, $\eta = 0.5$, and $C^R = 0.6$.

3.3.2. An overshooting effect of production delays

To provide more insight into how production delays lead to price fluctuations, we examine the price dynamics for different levels of τ. Figure 3.3 illustrates the price series for different levels of production delay when the initial state of the price is not in its steady state. When $\tau = 0$, there is no production delay, and demand and supply decisions are made at the same time. In this case, system (3.6) is "self-regulating" in the sense that the future dynamics are completely determined by the current price, and the left panel shows that the system is globally stable and that the price converges to its steady-state level monotonically.

When $\tau = 1$, although Proposition 3.3 shows that the system is still stable, the middle panel of Fig. 3.3 shows that the production delay gives rise to an overshooting effect.[10] More specifically, the initial price starts below its steady state, and initial demand is greater than initial supply, implying that the price will increase in following periods. However, when the price increases beyond its steady-state level at $t = 0.5$, demand is still greater than supply, and the price keeps increasing even if it is already greater than the steady state. Hence, the mismatch between demand and supply (or the *time inconsistency* between demand and supply decisions) generates an overshooting in price dynamics, which is followed by interchanges between periods of demand being greater than supply and periods of demand being less than supply. With a small time inconsistency, agents can easily adjust their demand and supply accordingly, and eventually, the system digests this inconsistency, leading to *consistency* between demand and supply and hence a stable price.

However, when $\tau = 10$, the time inconsistency is too large to be absorbed by the system, and the overshooting effect leads to long-lasting constant price fluctuations, as shown on the right panel of Fig. 3.3. In untabulated results, we also find that when the production delay increases, both the magnitude and the minimal period of the price fluctuations increase and that it hence becomes more difficult to harmonize demand and supply.

In all, we show that the overshooting effect is inherent to production delays. Without production delays, the system is linear, and hence there is no overshooting. With production delays, the system becomes nonlinear, and there is overshooting on price regardless of whether the system is stable. However, a change in other parameters cannot change the overshooting effect unless it alters the nonlinearity of the system. In the equilibrium models of Brock and Hommes (1997) and Gori et al. (2015), the price cycles resulting from the usage of naive predictors also reflect the overshooting effect.

3.3.3. The effect of switching intensity—the rational route to randomness

In this subsection, we study the role of the intensity of choice β. The following corollary shows that the steady state is stable at a low intensity of choice and becomes unstable when agents adjust their strategies quickly.

Corollary 3.4. *If $s > d/(1 - 2n^{R*})$, then the steady state (P^*, U^{R*}, U^{N*}) is locally asymptotically stable for $0 < \beta < \beta_0^*$, is unstable for $\beta > \beta_0^*$, and undergoes a Hopf bifurcation at $\beta = \beta_0^*$, where β_0^* is given by (A.9).*

[10] We use the term "overshooting" to highlight the nonmonotonic price-adjustment path, as illustrated in the middle and right panels of Fig. 3.3.

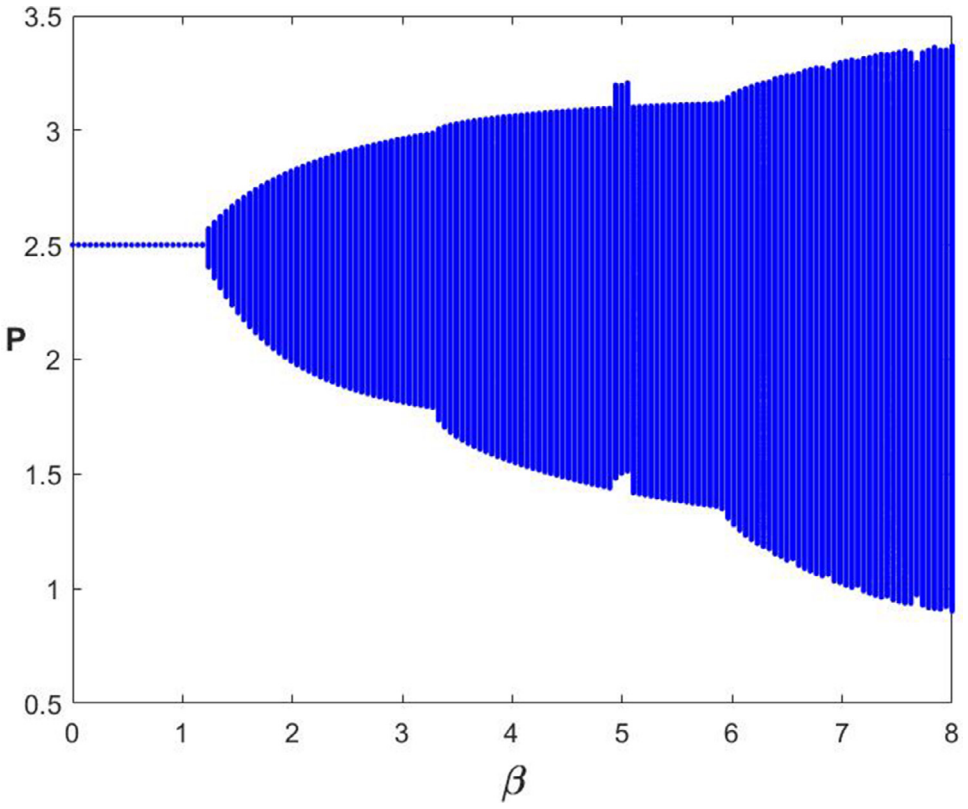

Fig. 3.4. The bifurcation diagram of the price with respect to β. Here $\tau = 10$, $\alpha = 1$, $A = 10$, $d = 1$, $s = 3$, $\eta = 0.5$, and $C^R = 0.6$. The steady state is $(P^*, U^{R*}, U^{N*}) = (2.5, 8.8, 9.4)$.

Brock and Hommes (1997) find that when the switching intensity is high, chaotic price behavior arises in their discrete-time cobweb model with perfect foresight versus naive expectations due to homoclinic bifurcations associated with saddle points. In the following analysis, we numerically verify that chaotic price behavior also arises in our continuous-time cobweb-type model with population evolutions.

Figure 3.4 illustrates the bifurcation diagram of the market prices with respect to β. The steady state is stable for a low intensity of choice $\beta < \beta_0^* (= 1.2)$ and becomes unstable as β increases. The price regularly fluctuates around its steady-state level for a low $\beta > \beta_0^*$. However, a further increase in β leads to secondary and even tertiary bifurcations of the periodic solutions, associated with more complex price behavior.

Figure 3.5 examines the price dynamics for large β ($\beta = 1 \times 10^6$). In this case, the price builds up slowly but crashes suddenly. However, most of the time (during the buildup of prices), most agents choose the naive predictor, leading the price to cyclically depart from the steady-state value. When the deviation of the price from the fair value is sufficiently large, the net profit associated with the naive predictor becomes lower than that associated with the perfect-foresight predictor, and with the high switching intensity, agents suddenly switch to the perfect-foresight predictor. This in turn leads to the sudden price crash. Figure 3.6 further illustrates the phase plot. It clearly shows that the price builds up slowly in association with increases in $U^R - U^N$ and then suddenly crashes when $U^R - U^N$ is sufficiently large.

The phenomena of slow buildup and sudden crash illustrated in Figs. 3.5-3.6 are driven mainly by the memory strength η. When $\eta \to 0$, the fitness measures U_t^i have a tendency to weight all past profits from a strategy equally; hence, we call this case the long-memory limit. In this limit, system (3.6) can be cast in the mold of a fast–slow system, with the price dynamics of the fast subsystem and the performance difference $U^R - U^N$ of the slow subsystem. Therefore, the performance difference and the market fraction move slowly even if the price fluctuates widely, as illustrated in Figs. 3.5-3.6. Appendix D shows that in the limit $\eta \to 0$, the price subsystem undergoes a Hopf bifurcation for a certain value D^* of the performance difference. For small η, the system dynamics are then close to the stable attractors of the price subsystem. Figure 3.6 can now be interpreted as follows: the bifurcating value of the performance difference D^* is close to the lower bound of the value of $U_t^R - U_t^N$. There, the central equilibrium $(P_t, P_{t-\tau}) = (P^*, P^*)$ destabilizes and the price dynamics start to follow the Hopf invariant circle. Along the resultant periodic dynamics, the perfect-foresight predictor has a performance advantage, which increases $U_t^R - U_t^N$ and lets the dynamics tend along the ever-increasing Hopf circles. When the performance difference is approximately 0, the perfect-foresight predictor takes over and forces the dynamics back to the $(P_t, P_{t-\tau}) = (P^*, P^*)$ axis. However, the naive predictor, being cheaper, takes over again, and the cycle repeats.

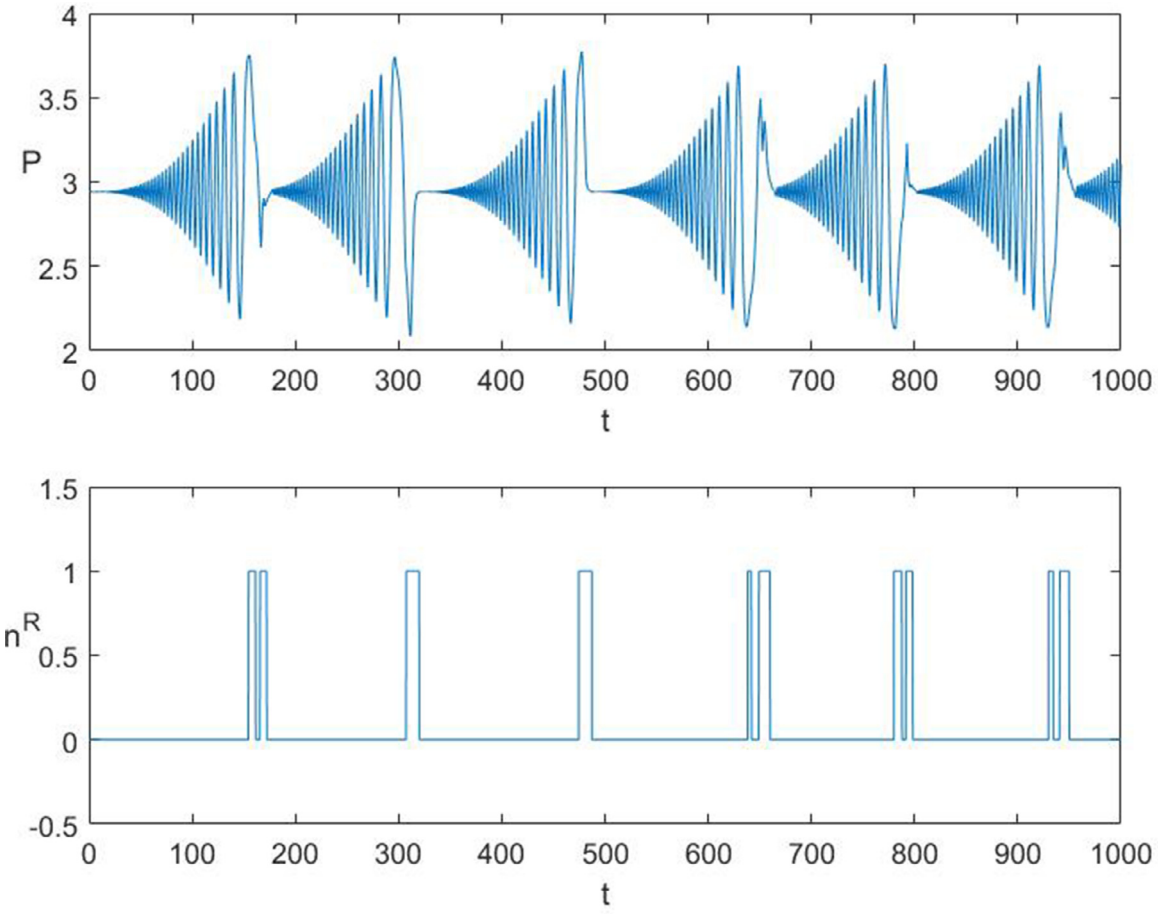

Fig. 3.5. The time series of the price (upper panel) and the market fraction of perfect-foresight traders (lower panel). Here, $\tau = 10$, $\alpha = 1$, $A = 10$, $d = 1$, $s = 3$, $\eta = 0.5$, $C^R = 0.6$, and $\beta = 1 \times 10^6$.

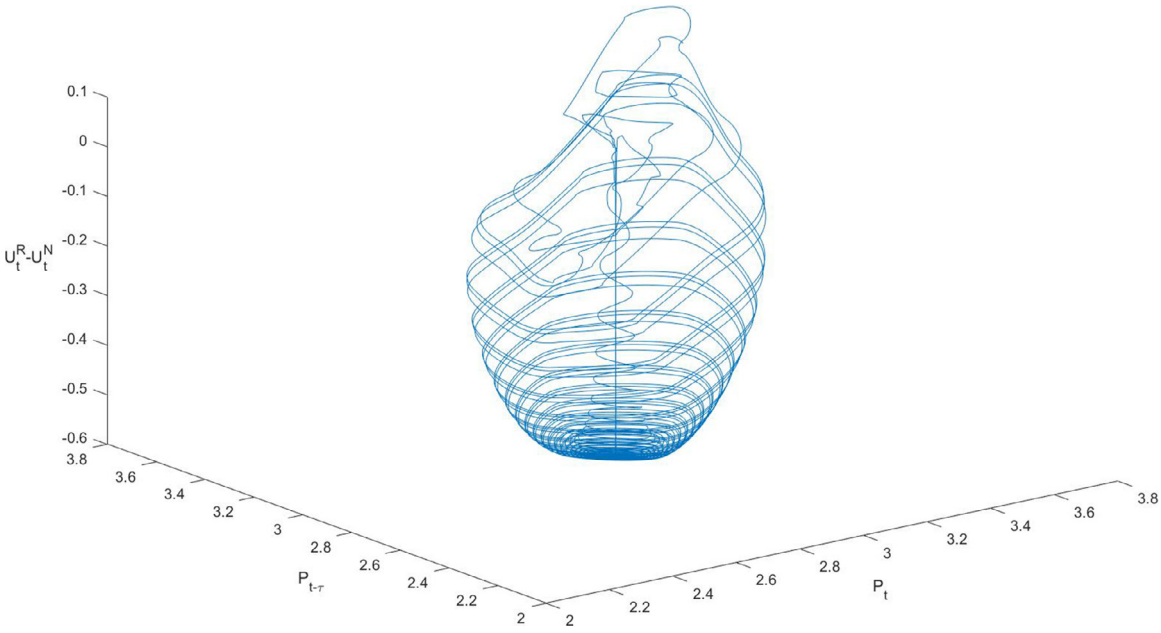

Fig. 3.6. The phase plots of $(P_t, P_{t-\tau}, U_t^R - U_t^N)$. Here, $\tau = 10$, $\alpha = 1$, $A = 10$, $d = 1$, $s = 3$, $\eta = 0.5$, $C^R = 0.6$, and $\beta = 1 \times 10^6$.

Moreover, Figs. 3.5-3.6 show that the price series is erratic. Although the price experiences booms and crashes repeatedly, the attractor is not regular, and the period of each "price cycle" is different, suggesting chaotic price behavior. This chaotic behavior is the outcome of a high intensity of choice β. In fact, Corollary 3.4 shows that the steady state becomes unstable for a high β. However, since every point in the segment $S = \left\{(P, U^R, U^N) |\ P = P^*, -\infty \le U^R, U^N \le \infty\right\}$ is mapped onto the steady state, there always exists a stable manifold of the steady state that contains S, implying that the unique steady state (P^*, U^{R*}, U^{N*}) is a saddle point. Let us consider a limiting case $\beta \to \infty$ such that agents switch infinitely fast between the two predictors. All firms use the naive (perfect-foresight) predictor whenever $U^N > U^R$ ($U^R > U^N$). For an initial state with all firms using the naive predictor, since the initial state lies in the unstable manifold of the steady state, the price cyclically departs from the steady-state price. As long as the deviation of the price from its steady state is large enough that $U^R > U^N$, all firms immediately switch to the perfect-foresight predictor, and the price suddenly converges to its steady state. After this, once the orbit lies in the stable manifold of the steady state, the system converges to the saddle-point steady state. Adding a small amount of noise to the system with $\beta \to \infty$ would lead to very irregular price fluctuations, which in fact are very similar to the fluctuations with large but finite values of β. Hence, when the intensity of choice is high, the system is close to having homoclinic orbits. This phenomenon is illustrated by the price time series in Fig. 3.5: once the price deviation from its steady state is large, all firms switch to the perfect-foresight predictor, leading to a sudden price drop to its steady state. This verifies the rational route to randomness of Brock and Hommes (1997) in our infinite-dimensional economy.

Technically, Brock and Hommes (1997) demonstrate, by showing the existence of "horseshoes," that for their finite-dimensional discrete-time cobweb model, there can be no homoclinic intersection between the stable and unstable manifolds of the steady state for low values of β while there must be homoclinic bifurcations associated with the saddle points for high values of β. However, the proof for our delay differential system (3.6) is much more involved because the time delay leads to infinite dimensions.[11] In this paper, we numerically examine chaotic price dynamics. To the best of our knowledge, this is the first numerical example of chaotic dynamics in an infinite-dimensional economy.

Numerical simulations (not reported here) show that the chaotic behavior is driven mainly by a high switching intensity rather than a large production delay in the sense that the price dynamics still exhibit regular cycles even for a large production delay as long as β is small. Increases in τ only enlarge the periods of price fluctuations.

3.4. Belief distributions

In the previous subsections, we focused on the delay impact by considering two beliefs. In this section, we extend the model to a case with a large belief set to examine the impact of belief distributions on price dynamics.

There are an infinite number of predictors over $[0, \tau]$, and the predictor indexed by i is given by

$$H^i_{t-\tau} = P_{t-i}, \qquad i \in [0, \tau]. \tag{3.8}$$

Therefore, in each time period, agents' beliefs follow a distribution over the predictor set, and (3.8) reflects the belief distribution at time $t - \tau$. One can also interpret this distribution as a (delay-dependent) technology distribution; in this case, different technologies require that firms using the naive predictors form their predictions at different points in time.[12]

Then the total supply at time t is given by

$$\sum nS = \int_0^\tau n^i_{t-\tau} S(H^i_{t-\tau}) di = s \int_0^\tau n^i_{t-\tau} P_{t-i} di, \tag{3.9}$$

where $n^i_{t-\tau} di$ is the fraction of agents who use predictor H^i at time $t - \tau$, satisfying $\int_0^\tau n^i_{t-\tau} di = 1$, and the price process is given by

$$\dot{P}_t = \alpha\left(A - dP_t - s \int_0^\tau n^i_{t-\tau} P_{t-i} di\right). \tag{3.10}$$

System (3.10) is governed by a differential system with distributed delays. At any time t, n^i_t can be regarded as the density of the delay distribution because $\int_0^\tau n^i_t di = 1$. When $\tau = 0$, all agents have perfect-foresight beliefs (atomic distribution), and the system becomes the ordinary differential equation (3.1). When $\tau = \infty$, beliefs are distributed over all historical prices. For the general continuous-time cobweb-type model (3.10) with an infinite number of beliefs, stability can be analyzed once the density of the delay distribution is specified. In the following analysis, we first show that the price dynamics can be significantly affected by the belief distributions via some simple examples, and then, we demonstrate that different price dynamics in turn can also lead to different belief distributions.

[11] Lani-Wayda and Walther (1995, 1996) show that delay differential systems have chaotic trajectories close to the homoclinic orbit when the set of the homoclinic orbit is rich enough. The idea is as follows. It can be shown that the homoclinic orbit is a hyperbolic set (Steinlein and Walther, 1990). Then, shadowing theorem (pp.18–19 Ott, 1993) implies that chaotic trajectories close to the homoclinic orbit exist.

[12] We are greatly indebted to an anonymous referee who emphasized this point and provided us with many other very helpful comments.

3.4.1. Examples of static belief distributions

Before studying dynamic populations, we first examine some static distributions in which n_t^i is given exogenously to provide a better understanding of the impact of belief distributions. The first example is a system with uniformly distributed agents. In this case, the total supply reduces to $\frac{1}{\tau}\int_0^\tau (sH_{t-\tau}^i)di = \frac{s}{\tau}\int_{t-\tau}^t P_u du$, and the price is given by

$$\dot{P}_t = \alpha\left(A - dP_t - \frac{s}{\tau}\int_{t-\tau}^t P_u du\right). \tag{3.11}$$

The local stability of system (3.11) is characterized by the following proposition.

Proposition 3.5. *System (3.11) has a unique steady-state price $P^* = A/(d+s)$, which is locally asymptotically stable under*

$$(\mathbf{C}) = \{s < d/x^*\}\bigcup\{\tau_0^{***} \geq (s-d)/(\alpha d^2)\}\bigcup\{0 \leq \tau < \tau_0^{***}\}\bigcup\{\tau > \tilde{\tau}^{***}\} \tag{3.12}$$

(where $x^* = \max\{-\sin x/x; x > 0\}(\approx 0.2172)$ and τ_0^{***} and $\tilde{\tau}^{***}$ are defined in Appendix A.5) and unstable under

$$\overline{(\mathbf{C})} = \{s \geq d/x^*\}\bigcap\{\tau_0^{***} < (s-d)/(\alpha d^2)\}\bigcap\{\tau_0^{***} < \tau < \tilde{\tau}^{***}\}, \tag{3.13}$$

which is the complementary set of (**C**).

The stable condition (**C**) in (3.12) shows that system (3.11) is stable for both a small τ and a large τ while the results for a medium τ are mixed depending on the other parameters. However, unlike in the discrete-delay case in Sections 3.2–3.3, a large delay in the distributed-delay system plays a stabilizing role. This is because moving average processes, such as (3.11), generally have positive (negative) feedback for small (large) values of τ (He et al., 2009). In addition, (3.12) shows that the system is stable for small values of s or large values of d. For example, the system is always stable when $d > 0.2172s$. This is consistent with Proposition 3.3, which shows the destabilizing role of s and stabilizing role of d.

The unstable condition $\overline{(\mathbf{C})}$ in (3.13) is unlikely to be satisfied, implying that P^* is stable for most (if not all) cases. This is inconsistent with the first general local instability theorem proposed in Brock and Hommes (1997), which shows that the system is unstable when beliefs are uniformly distributed over a finite expectation set. In fact, the infinite predictor set in the continuous-time setup includes almost-perfect-foresight expectations, which are inherently excluded by the discrete-time models. The price movements become predictable under these expectations, and countercyclical production responses can smooth out market fluctuations, causing the cycle to disappear.[13] As a result, the steady-state price P^* becomes locally stable by violating Brock and Hommes (1997)'s assumption (Assumption A2 on pp. 1064) that the steady-state price is locally unstable when agents are uniformly distributed over the predictor space.

Appendix B studies two more examples of static distributions, including a linear fitness function case and a gamma distribution. The linear fitness function case features multiple stability switchings in the sense that an increase in τ can destabilize the price while a further increase may stabilize an otherwise unstable price.[14] When beliefs follow a gamma distribution, the system is always stable. To sum up, we show that agents' belief distributions significantly affect market stability. Different distributions lead to very different price dynamics, and nonlinear distributions can give rise to complex price behavior. This is similar to the notion of a high limit introduced by Brock et al. (2005) and Hommes and Wagener (2010) to study evolutionary heterogeneous market systems with many different strategy types. They show that the initial distribution of strategies plays a decisive role in market stability. See also Diks and van der Weide (2005) for a related approach.

3.4.2. Population evolution

Now, we study dynamic belief distributions when agents update their beliefs based on the relative net benefits. It follows from (2.2) that the market fraction of agents with belief i at time t is given by $n_t^i di = \frac{e^{\beta U_t^i}di}{\int_0^\tau e^{\beta U_t^i}di}$, where U_t^i, the fitness function associated with belief i at time t, is governed by $\dot{U}_t^i = \eta[\frac{s}{2}P_t(2P_t - P_{t-i}) - C^i - U_t^i]$. The constant information cost C^i is assumed to decrease in i; that is, agents have to pay more to obtain predictors closer to the one with perfect foresight. The fitness function can be rewritten as

$$U_t^i = \frac{s\eta}{2}\int_0^t e^{\eta(u-t)}P_u(2P_u - P_{u-i})du + U_0^i e^{-\eta t} - C^i(1-e^{-\eta t}). \tag{3.14}$$

Then, the total supply is given by $\sum nS = s\frac{\int_0^\tau e^{\beta U_{t-\tau}^i}P_{t-i}di}{\int_0^\tau e^{\beta U_{t-\tau}^i}di}$, and hence, the price process is given by

$$\dot{P}_t = \alpha\left(A - dP_t - s\frac{\int_0^\tau e^{\beta U_{t-\tau}^i}P_{t-i}di}{\int_0^\tau e^{\beta U_{t-\tau}^i}di}\right), \tag{3.15}$$

[13] In other words, the inconsistency between the results in the continuous-time model and discrete-time models is due to the difference between continuous distributions and discrete distributions.

[14] Similarly, the asset-pricing system with the same characteristic equation form developed in He et al. (2009) also undergoes multiple stability switchings within $[\tau_0, \tilde{\tau}]$, while it becomes stable outside this interval.

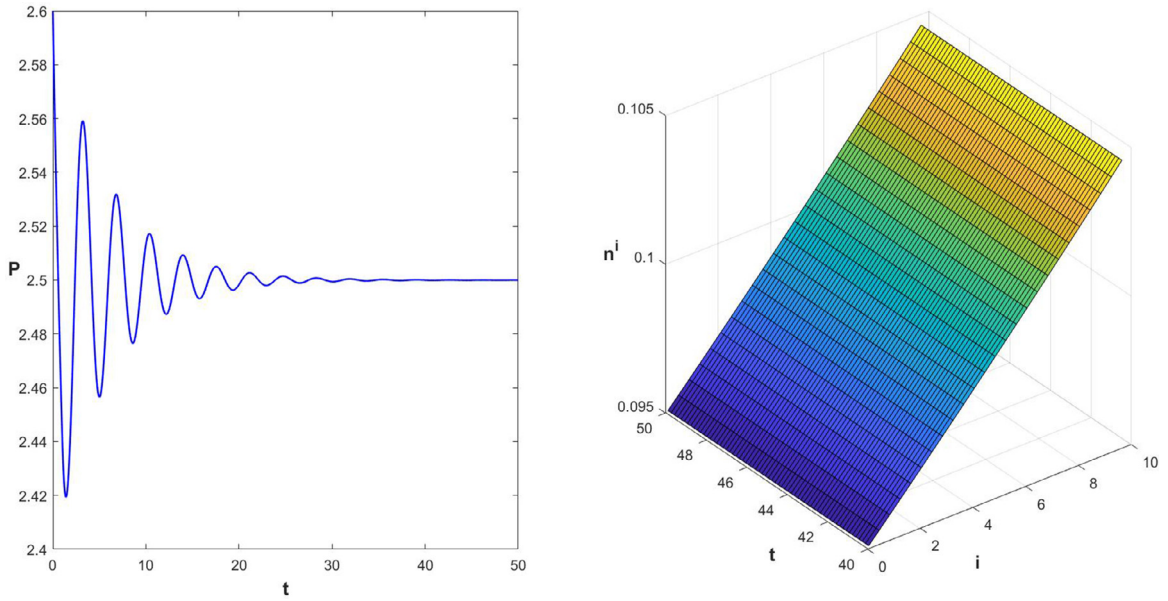

Fig. 3.7. The left panel illustrates the price time series, and the right panel illustrates the dynamic belief distributions. Here, $\beta = 1$, $\tau = 10$, $\alpha = 1$, $A = 10$, $d = 1$, $s = 3$, $\eta = 0.5$, $c_1 = 1$, and $c_2 = 0.1$.

where U_t^i is given by (3.14). The general model (3.15) is governed by a nonautonomous delay differential equation, and currently there is no stability and bifurcation theory for this type of system. However, we can discuss the stability in several limiting cases, which provide more insight into the effect of belief distributions.

Proposition 3.6.

(1) *System (3.15) has a unique steady-state price* $P^* = A/(d+s)$.
(2) *If* $C^i = 0$ *or* $\beta = 0$, *then* P^* *is locally asymptotically stable under* (**C**) *and unstable under* $\overline{(\mathbf{C})}$, *where conditions* (**C**) *and* $\overline{(\mathbf{C})}$ *are defined in (3.12) and (3.13), respectively.*
(3) *The steady-state price* P^* *is unstable when* $\tau > \tau_0^{**}$ *and* β *is sufficiently large, where* τ_0^{**} *is defined in Proposition 3.2.*

Note that we do not specify the function of the information cost C^i but only assume that it decreases in index i in Proposition 3.6. The conditions (**C**) and $\overline{(\mathbf{C})}$ have been discussed in Section 3.4.1. There are several observations from Proposition 3.6. First, although agents adjust their predictors based on an infinite set of beliefs over time, (3.15) shares the same unique steady-state price $P^* = A/(d+s)$ as systems (3.1), (3.3) and (3.6). The condition $\overline{(\mathbf{C})}$ is unlikely to be satisfied (see Section 3.4.1 or Appendix A.5). Hence, part (2) of Proposition 3.6 shows that when there is no information cost, the tension between stabilizing and destabilizing forces causes the dynamics to almost surely settle into the steady-state price for most (if not all) values of the time delay τ. Intuitively, the market without information costs is dominated by beliefs close to perfect foresight with small delays, which play stabilizing roles. As a result, the system tends to be stable even in the presence of population evolution and an infinite number of beliefs.

Second, when the intensity of choice $\beta = 0$, there is no belief switching, and heterogeneous agents are equally distributed over the space of predictors. The price dynamics are the same as in system (3.11).

Finally, because agents have to pay more to obtain predictors closer to perfect foresight, part (3) of Proposition 3.6 shows that for large values of τ, the steady-state price P^* is stable for small values of β but becomes unstable when the intensity of choice β is sufficiently high. This is consistent with the second general local instability theorem in Brock and Hommes (1997).

Now, we numerically examine price behavior and dynamic belief distributions. We consider a linear cost function $C^i = c_1 - c_2 i$ ($c_1, c_2 \geq 0$). In the left panel of Fig. 3.7, the price is stable when the intensity of choice β is low. The right panel of Fig. 3.7 shows that as time t increases, the corresponding belief distribution becomes "stationary" in the sense that it eventually converges to a fixed distribution and does not change over time. Equation (3.14) implies that U^i in the steady state increases in i. Thus, in the steady state, the market fraction of agents with i-belief increases with i, as illustrated in the right panel of Fig. 3.7.

The upper left panel of Fig. 3.8 illustrates that when β is large, the system becomes unstable, and the price (the solid blue line) fluctuates around the steady-state level (the dashed red line) in a cyclic way. We plot the fitness functions for two extreme beliefs, $i = 0$ and $i = \tau$, as well as their steady-state levels, in the upper right panel of Fig. 3.8. It shows that the fitness functions periodically fluctuate in association with the price fluctuation; however, the steady-state fitness of belief

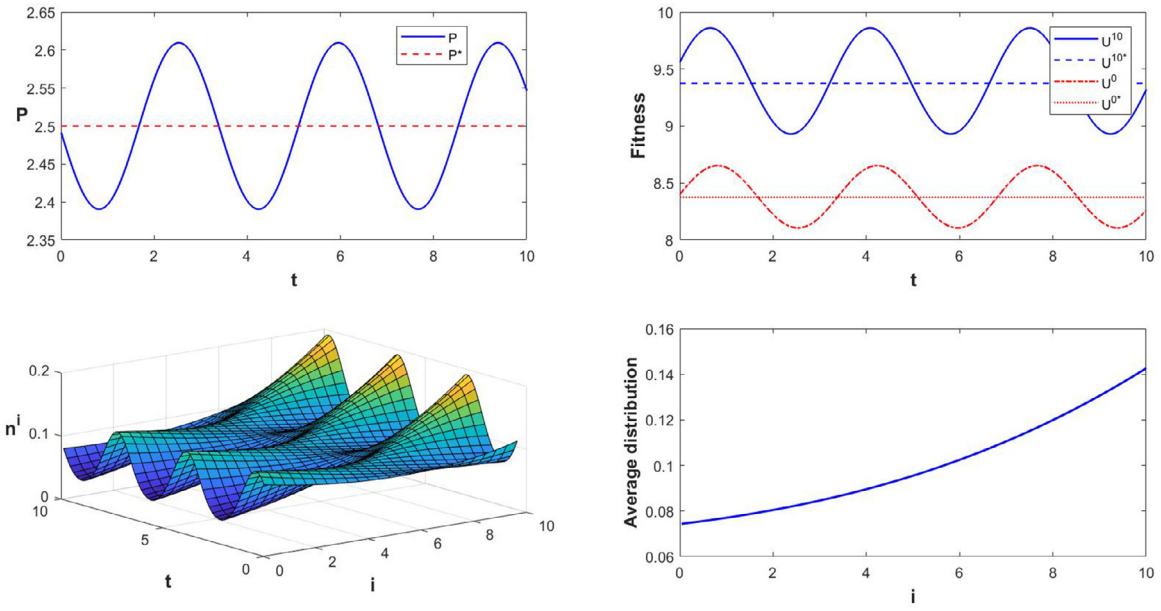

Fig. 3.8. The upper panel illustrates the price time series (left panel) and fitness functions for beliefs $i = 0$ and $i = \tau$ (right panel). The lower left panel illustrates the dynamic belief distributions, and the lower right panel illustrates the average belief distribution over time. Here, $\beta = 5$, $\tau = 10$, $\alpha = 1$, $A = 10$, $d = 1$, $s = 3$, $\eta = 0.5$, $c_1 = 1$, and $c_2 = 0.1$.

$i = \tau$ is greater than that of $i = 0$. The lower left panel plots the dynamic belief distributions over time. It shows that when the system is unstable, the belief distribution becomes "nonstationary" and fluctuates as the price fluctuates. The dynamic population fractions seesaw over time. The lower right panel of Fig. 3.8 plots the average distribution over time. It clearly shows that the population fraction increases with i on average. Therefore, more agents use the beliefs with lower costs, consistent with the case in the right panel of Fig. 3.7. In addition, under the same set of parameters, system (3.6) with two beliefs is stable. Therefore, when producers use more beliefs, the market tends to become less stable.

In all, we show that consistent with the main findings in Section 3.3, when agents are allowed to update their beliefs based on a large belief set, both production delays and the intensity of choice play destabilizing roles in a more general setup.

4. Conclusion

Most of the cobweb models developed in the literature are in a discrete-time setup. In this setup, the impacts of nonlinear demand/supply curves and adaptive behavior on market stability have been widely studied, while the impacts of production delays and belief distributions on market stability have not been well understood due to the problem of high-dimensional systems. This paper develops a continuous-time framework to study the joint impact of lagged prices and adaptive behavior of producers. The resultant delay differential equations provide a unified approach to systematically study the impact of lagged prices and belief distributions through a time-delay parameter.

We find that the time inconsistency between demand and supply due to production delays inherently generates an overshooting effect in prices. Large production delays give rise to price fluctuations, even with a low intensity of choice. We provide results consistent with the *rational route to randomness* of Brock and Hommes (1997) in an infinite-dimensional economy. We also show that different belief distributions may result in very different price dynamics and that stable (unstable) prices are typically associated with stationary (nonstationary) belief distributions.

Many heterogeneous agent models, including our model, assume that agents switch among predictors, which are heterogenous in terms of both cost and "quality", based mainly on their past performance. This setup helps understand the different roles played by different predictors in the market. However, in this setup, if agents who recently purchased costly information decide to switch their predictors, they will completely discard the recent information that could be still useful in predicting prices in the near future. To account for this, one could allow the agents to strategically choose the predictors by minimizing costs and optimally reusing recently purchased information. We leave this for future research.

Declaration of Competing Interest

None.

Acknowledgment

We would like to thank Daniel Houser (the editor), an Associate Editor, two anonymous referees, Xue-Zhong He, Chuncheng Wang, and conference and seminar participants at the Inaugural Workshop on Complex Information and Financial Market Dynamics, Harbin Institute of Technology, Southwestern University of Finance and Economics, and University of Technology Sydney for helpful comments and suggestions. Financial support from the Australian Research Council (Project ID: DE180100649) is gratefully acknowledged. All remaining errors are ours.

Appendix A. Proofs

A1. Proof of Proposition 3.1

It is easy to verify that (3.1) has a unique steady state $P^* = A/(d+s)$. It follows from (3.1) that

$$P_t = (P_0 - P^*)e^{-\alpha(d+s)t} + P^*,$$

which converges to P^* as $t \to \infty$.

A2. Proof of Proposition 3.2

The characteristic equation of system (3.3) in its unique steady state $P^* = A/(d+s)$ is given by

$$\lambda + \alpha d + \alpha s e^{-\lambda\tau} = 0, \tag{A.1}$$

which has no zero eigenvalue.

For $\tau = 0$, Appendix A.1 has shown that the steady state P^* is asymptotically stable and therefore the root of (A.1) has a negative real part. Let $\lambda = i\omega(\omega > 0)$ be a root of (A.1). Substituting it into (A.1) and separating the real and imaginary parts yield

$$\alpha d + \alpha s\cos\omega\tau = 0, \quad \omega - \alpha s\sin\omega\tau = 0, \tag{A.2}$$

which lead to

$$\omega^2 + \alpha^2 d^2 = \alpha^2 s^2. \tag{A.3}$$

If $s \le d$, then (A.3) has no solution. It is known that as τ varies, the sum of the multiplicities of roots of (A.1) in the open right half-plane can change only if a root appears on or crosses the imaginary axis (see Li and Wei, 2009). Therefore, all roots of (A.1) have negative real parts for all $\tau \ge 0$ when $s \le d$. This implies the local stability of system (3.3). If $s > d$, then $\omega^{**} = \alpha\sqrt{s^2 - d^2}$. Substitute it into the first equation of (A.2), and we have

$$\tau_n^{**} = [\cos^{-1}(-d/s) + 2n\pi]/\omega^{**}, \quad n = 0, 1, 2, \cdots. \tag{A.4}$$

We can verify the transversal condition $\frac{\partial \mathrm{Re}\{\lambda\}}{\partial\tau}\Big|_{\lambda=i\omega^{**}} = \omega^{**2} + \alpha d^2 > 0$, implying that all roots that cross the imaginary axis at $i\omega^{**}$ do so from left to right as τ increases. Thus, stability is lost at $\tau = \tau_0^{**}$ and cannot be regained as τ increases.

Furthermore, after substituting ω^{**} into τ_0^{**}, we can verify that

$$\begin{aligned}
\frac{\partial\tau_0^{**}}{\partial d} &= \frac{\sqrt{s^2-d^2}\left[s^2-d^2+s\sqrt{s^2-d^2}\cos^{-1}(-d/s)\right]}{\alpha A(s-d)(s^2-d^2)\sqrt{s^2-d^2}} > 0,\\
\frac{\partial\tau_0^{**}}{\partial s} &= -\frac{d}{s}\frac{\partial\tau_0^{**}}{\partial d} < 0, \quad \frac{\partial\tau_0^{**}}{\partial\alpha} = -\frac{\cos^{-1}(-d/s)}{\alpha^2 P^*\sqrt{s^2-d^2}} < 0.
\end{aligned}$$

They show that τ_0^{**} increases with d but decreases with s and α. In this sense, b plays a stabilizing role but s and α play destabilizing roles in the market.

A3. Proofs of Proposition 3.3 and Corollary 3.4

The characteristic equation of system (2.7) in the unique steady state $(P^*, U^{R*}, U^{N*}) = (\frac{A}{d+s}, \frac{sA^2}{2(d+s)^2} - C^R, \frac{sA^2}{2(d+s)^2})$ is given by

$$(\lambda+\eta)^2\left[\lambda + \alpha(d + sn^{R*}) + \alpha s(1-n^{R*})e^{-\lambda\tau}\right] = 0, \tag{A.5}$$

which has no zero eigenvalue.

The first term on the left-hand side of (A.5) implies two negative eigenvalues $\lambda_{1,2} = -\eta < 0$. Thus, we need to consider only the term in the square brackets

$$\lambda + \alpha(d + sn^{R*}) + \alpha s(1-n^{R*})e^{-\lambda\tau} = 0. \tag{A.6}$$

We have the following equations by substituting $\lambda = i\omega$ into (A.6),

$$\begin{aligned} \alpha(d + sn^{R*}) + \alpha s(1 - n^{R*})\cos\omega\tau &= 0, \\ \omega - \alpha s(1 - n^{R*})\sin\omega\tau &= 0, \end{aligned}$$

leading to

$$\omega^2 = \alpha^2[s^2(1 - n^{R*})^2 - (d + sn^{R*})^2]. \tag{A.7}$$

Equation (A.7) cannot hold if $s \le d/(1 - 2n^{R*})$.

When $s > d/(1 - 2n^{R*})$, following the same method as in Appendix A.2, the Hopf bifurcation values are given by

$$\tau_n^* = \frac{1}{\omega^*}\left[\cos^{-1}\left(-\frac{d + sn^{R*}}{s(1 - n^{R*})}\right) + 2n\pi\right], \quad n = 0, 1, 2, \cdots, \tag{A.8}$$

where $\omega^* = \alpha\sqrt{s^2(1 - n^{R*})^2 - (d + sn^{R*})^2}$ and the transversal condition satisfies $\frac{\partial \mathrm{Re}\{\lambda\}}{\partial \tau}\Big|_{\lambda = i\omega^*} > 0$.

Furthermore, the Hopf bifurcation values with respect to β are governed by

$$\left\{\frac{b[1 - \tanh(-\beta C^R/2)]}{d + s\tanh(-\beta C^R/2)}\cos\left[\alpha\sqrt{s^2(1 - \tanh(-\beta C^R/2))^2 - (d + s\tanh(-\beta C^R/2))^2}\tau\right]\right\}^2 = 1. \tag{A.9}$$

Equation (A.9) cannot be explicitly solved, but the existence of solutions $\beta_n^*(\tau)$ can be guaranteed by (A.8). The transversal condition satisfies $\frac{\partial \mathrm{Re}\{\lambda\}}{\partial \beta}\Big|_{\lambda = i\omega^*} > 0$, implying that the system becomes unstable for $\beta > \beta_0^*(\tau)$.

A4. Proof of Proposition 3.5

See Appendix A.5 for the proof of a general case.

A5. Proof of Proposition 3.6

It is easy to verify that (3.15) has a unique steady-state price $P^* = A/(d + s)$. The proof of Proposition 3.6 follows two steps—without/with an information cost.

First, we consider no information cost, $C^i = 0$. In this case, U_t^i shares the same form as (3.14) for all i. If we consider that they start from the same initial value, then U_t^i has the same value at time t for all i. Therefore, $U_t^i = U_t$ is independent of i, and hence, system (3.15) reduces to

$$\dot{P}_t = \alpha\left[A - dP_t - s\frac{\int_{t-\tau}^t \exp\{\beta U_{t-\tau}\}P_u du}{\int_{t-\tau}^t \exp\{\beta U_{t-\tau}\}du}\right] = \alpha\left[A - dP_t - \frac{s}{\tau}\int_{t-\tau}^t P_u du\right]. \tag{A.10}$$

To find the stability condition of system (3.15) when $C^i = 0$, it suffices to derive the stability condition for (A.10). The characteristic equation of system (A.10) in the steady state P^* is given by

$$\lambda + \alpha d + \frac{\alpha s}{\lambda\tau}(1 - e^{-\lambda\tau}) = 0, \tag{A.11}$$

which has no zero eigenvalue.

Substituting $\lambda = i\omega(\omega > 0)$ into (A.11) and separating the real and imaginary parts yield

$$\begin{aligned} -\omega^2 + \tfrac{\alpha s}{\tau}(1 - \cos\omega\tau) &= 0, \\ \alpha d\omega + \tfrac{\alpha s}{\tau}\sin\omega\tau &= 0. \end{aligned} \tag{A.12}$$

Let $x^* = \max\{-\sin x/x; x > 0\}(\approx 0.2172)$. When $s < d/x^*$, the two functions $y_1 = -d/sx$ and $y_2 = \sin x$ have no intersection for $x > 0$; hence, the second equation of (A.12) cannot be true, and (A.11) has no pure imaginary root. Correspondingly, (A.11) has no root appearing on the imaginary axis. In addition, (A.11) has a unique negative eigenvalue $\lambda = -\alpha(d + s) < 0$ for $\tau = 0$. Therefore, all roots of (A.11) have negative real parts for all $\tau \ge 0$ when $s < d/x^*$, which leads to the local stability of system (3.15).

Now, we consider the case of $s \ge d/x^*$. It follows from (A.12) that

$$\omega^2 = \alpha\left(\frac{2s}{\tau} - \alpha d^2\right). \tag{A.13}$$

When $\tau \ge 2s/(\alpha d^2)$, (A.13) has no solution, implying that $\lambda = i\omega$ is not an eigenvalue. Hence, there is no stability switching for $\tau \ge 2s/(\alpha d^2)$. Substituting $\lambda = \mathrm{Re}\{\lambda\} + i\,\mathrm{Im}\{\lambda\}$ into (A.11) and separating the real and imaginary parts yield

$$\begin{aligned} \mathrm{Re}^2\{\lambda\} - \mathrm{Im}^2\{\lambda\} + \alpha d\,\mathrm{Re}\{\lambda\} + \tfrac{\alpha s}{\tau}\left(1 - e^{-\mathrm{Re}\{\lambda\}\tau}\right)\cos\mathrm{Im}\{\lambda\}\tau &= 0, \\ 2\,\mathrm{Re}\{\lambda\}\,\mathrm{Im}\{\lambda\} + \alpha d\,\mathrm{Im}\{\lambda\} + \tfrac{\alpha s}{\tau}e^{-\mathrm{Re}\{\lambda\}\tau}\sin\mathrm{Im}\{\lambda\}\tau &= 0. \end{aligned} \tag{A.14}$$

When $\tau \to \infty$, if there exists a root λ with $\mathrm{Re}\{\lambda\} > 0$, then (A.14) reduces to

$$\begin{aligned} \mathrm{Re}^2\{\lambda\} - \mathrm{Im}^2\{\lambda\} + \alpha d\,\mathrm{Re}\{\lambda\} &= 0, \\ 2\,\mathrm{Re}\{\lambda\}\,\mathrm{Im}\{\lambda\} + \alpha d\,\mathrm{Im}\{\lambda\} &= 0, \end{aligned}$$

which cannot hold. Thus, (A.11) has all roots with negative real parts when $\tau \to \infty$, implying that the steady state P^* is asymptotically stable for $\tau \geq 2s/(\alpha d^2)$ when $s \geq d/x^*$. However, if $\tau < 2s/(\alpha d^2)$, by substituting (A.13) into the first equation of (A.12), we have

$$\frac{\alpha d^2 \tau}{s} - \cos\sqrt{2\alpha s\tau - \alpha^2 d^2 \tau^2} - 1 = 0. \tag{A.15}$$

(A.15) can have multiple solutions, as shown in He and Li (2015), and the number of solutions (A.15) increases as $\alpha d \to 0$.[15] Let τ_0^{***} be the minimum positive root of (A.15). Then, all the eigenvalues of (A.11) have negative real parts when $0 \leq \tau < \tau_0^{***}$. It can be easily verified that

$$\left.\frac{\partial \operatorname{Re}\{\lambda\}}{\partial \tau}\right|_{\tau=\tau_n^{***}} = \frac{\operatorname{Im}^2\{\lambda\}(\alpha s - \alpha d - \alpha^2 d^2 \tau_n^{***})}{\tau_n^{***}\{[\alpha d + \alpha s\cos(\operatorname{Im}\{\lambda\}\tau_n^{***})]^2 + [2\operatorname{Im}\{\lambda\} - \alpha s \sin(\operatorname{Im}\{\lambda\}\tau_n^{***})]^2\}},$$

which is positive for $\tau_n^{***} < (s-d)/(\alpha d^2)$ and negative for $\tau_n^{***} > (s-d)/(\alpha d^2)$. As a result, a stable system cannot become unstable as τ increases in $\left[(s-d)/(\alpha d^2), +\infty\right)$. In all, when $\tau_0^{***} \geq (s-d)/(\alpha d^2)$, system (3.15) is stable for all $\tau \geq 0$; when $\tau_0^{***} < (s-d)/(\alpha d^2)$, then there exists a $\tilde{\tau}^{***}$, which is a solution of (A.15) and satisfies $(s-d)/(\alpha d^2) < \tilde{\tau}^{***} < 2s/(\alpha d^2)$, such that the steady state P^* is asymptotically stable for $0 \leq \tau_0^{***}$ or $\tau > \tilde{\tau}^{***}$, is unstable for $\tau_0^{***} < \tau < \tilde{\tau}^{***}$, and undergoes Hopf bifurcations at $\tau = \tau_0^{***}$ and $\tau = \tilde{\tau}^{***}$.

Notice that system (3.15) has the same characteristic Eq. (A.11) when $\beta = 0$ and hence has the same stability as in the case without an information cost. In all, we show that for $C^i = 0$ or $\beta = 0$, the steady-state price P^* is locally asymptotically stable under the condition

$$(\mathbf{C}) := \{s < d/x^*\} \bigcup \{\tau_0^{***} \geq (s-d)/(\alpha d^2)\} \bigcup \{0 \leq \tau < \tau_0^{***}\} \bigcup \{\tau > \tilde{\tau}^{***}\}$$

and unstable under the condition

$$\overline{(\mathbf{C})} = \{s \geq d/x^*\} \bigcap \{\tau_0^{***} < (s-d)/(\alpha d^2)\} \bigcap \{\tau_0^{***} < \tau < \tilde{\tau}^{***}\},$$

which is the complementary set of (**C**).

Second, we study the stability for sufficiently large values of β.[16] Applying variation of constants to (3.15), we have

$$P_t = e^{-\alpha dt}\left[P_0 + \int_0^t \left(\alpha A - \alpha s \frac{\int_0^\tau e^{\beta U^i_{u-\tau}} P_{u-i} di}{\int_0^\tau e^{\beta U^i_{u-\tau}} di}\right) e^{\alpha d u} du\right].$$

Suppose that P^* is stable for big β. As $t \to \infty$, we have

$$P_t \to e^{-\alpha dt}\left[P_0 + \int_0^t \left(\alpha A - \alpha s \frac{\int_0^\tau e^{\beta U^i_*} P_{u-i} di}{\int_0^\tau e^{\beta U^i_*} di}\right) e^{\alpha d u} du\right], \tag{A.16}$$

where U^i_* is the steady-state fitness when $P_t = P^*$. Notice that $\left(\int_0^\tau e^{\beta U^i_*} P_{u-i} di\right)/\left(\int_0^\tau e^{\beta U^i_*} di\right)$ is a weighted average of historical prices over $[u-\tau, u]$. Because C^i is a decreasing function of i, $U^i_* = sP^{*2}/2 - C^i$ increases in i. When $\beta \to \infty$, all the weights go to time $u-\tau$, and hence the weighted average of historical prices tends toward $P_{u-\tau}$. In this case, the price process reduces to (3.3), and Appendix A.2 has demonstrated that P_t cannot converge to P^* when $\tau > \tau_0^{**}$. There is a contradiction. Therefore, the steady state P^* cannot be stable for sufficiently large values of β when $\tau > \tau_0^{**}$.

Appendix B. Some examples of expectation distributions

B1. A linear fitness function

The second example is a linear fitness function $U_t^i - C^i = g - ci$, where g and c (≥ 0) are constants. The net fitness in this case is inversely proportional to the production delay, implying that the farther the predictor is from perfect foresight, the less net fitness it gains. Then, the total supply becomes

$$\sum nS = \frac{s}{a}\int_{t-\tau}^t \mathrm{e}^{-\beta c(t-u)} P_u du, \quad a = \frac{1 - \mathrm{e}^{-\beta c\tau}}{\beta c},$$

and hence the price process is given by

$$\dot{P}_t = \alpha\left(A - dP_t - \frac{s}{a}\int_{t-\tau}^t \mathrm{e}^{-\beta c(t-u)} P_u du\right). \tag{B.1}$$

[15] We refer readers to Appendix B.4 in He and Li (2015) for more properties on (A.15), including the number of bifurcations, stability switching and the dependence of the bifurcation values on the parameters.

[16] In general, (3.15) is a nonautonomous equation due to the information cost, and we cannot apply standard stability and bifurcation theory. Here, we discuss the stability for a special case when β is sufficiently large.

The price dynamics of system (B.1) are described by the following proposition.

Proposition B.1. *System (B.1) has a unique steady-state price $P^* = A/(d+s)$, which is locally asymptotically stable for $\tau < \tau_0$ or $\tau > \tilde{\tau}$, where τ_0 is the smallest Hopf bifurcation value determined by (B.2) and $\tilde{\tau}$ is defined in (B.5).*

Proof. The characteristic equation of (B.1) is given by

$$p(\lambda, \tau) + q(\lambda, \tau)e^{-\lambda\tau} = 0, \tag{B.2}$$

where

$$p(\lambda, \tau) = \lambda^2 + (\beta c + \alpha d)\lambda + \alpha d\beta c + \frac{\alpha s \beta c}{1 - e^{-\beta c \tau}},$$
$$q(\lambda, \tau) = -\frac{\alpha s \beta c}{1 - e^{-\beta c \tau}} e^{-\beta c \tau}.$$

It is easy to verify that (B.2) has two negative roots, $\lambda_1 = -\beta c < 0$ and $\lambda_2 = -\alpha(d+s) < 0$, when $\tau = 0$. Hence, system (B.1) is stable for $\tau < \tau_0$, where τ_0 is the smallest Hopf bifurcation value.

Denote

$$Q_t := \frac{1}{a}\int_{t-\tau}^{t} e^{-\beta c(t-u)} P_u du.$$

Then,

$$\dot{P}_t = \alpha(A - dP_t - bQ_t). \tag{B.3}$$

When $\tau \to \infty$, we have

$$\dot{Q}_t = \beta c(P_t - Q_t). \tag{B.4}$$

The characteristic equation of (B.3) and (B.4) is given by

$$\lambda^2 + (\beta c + \alpha d)\lambda + \beta c \alpha (d+s) = 0,$$

which has two negative roots. In addition, the geometric stability switch criteria shows that the system cannot undergo Hopf bifurcation when $\tau > \tilde{\tau}$ (He et al., 2009), where

$$\tilde{\tau} = \ln\left[1 + \frac{2\beta c \alpha s}{(\beta c + \alpha d)^2 + 2(\beta c + \alpha d)\sqrt{\beta c(\alpha d + \alpha s)}}\right]^{1/(\beta c)}. \tag{B.5}$$

Therefore, system (B.1) is stable for $\tau > \tilde{\tau}$. □

Proposition Appendix B.1 shows that the system can be stable for either small or large values of τ but may become unstable over $[\tau_0, \tilde{\tau}]$. With a certain set of parameters, the system can have multiple stability switchings in the sense that an increase in τ can destabilize the price while a further increase may stabilize an otherwise unstable price.

B2. Gamma-distributed expectations

We provide another example in which agents' beliefs follow a gamma distribution. The gamma-distributed delay was initially proposed by MacDonald (1978) and has been widely used in the mathematical biology literature (see Zuo and Song, 2015 for a recent survey). In this case, the system becomes

$$\dot{P}_t = \alpha\left[A - dP_t - s\int_0^{\infty} n_u P_{t-u} du\right], \tag{B.6}$$

where the market fraction n_t follows the gamma distribution

$$n_t = \frac{t^m e^{-t/\tau}}{\tau^{m+1} m!}, \tag{B.7}$$

where m is a nonnegative integer and $\tau > 0$ is a scale parameter.

System (B.6) has a unique steady-state price $P^* = A/(d+s)$. The characteristic equation of system (B.6) in the steady state P^* is given by

$$(\lambda + \alpha d)(\tau\lambda + 1)^{m+1} + \alpha s = 0. \tag{B.8}$$

In particular, when $m = 0$, the population distribution becomes $n_t = \frac{1}{\tau} e^{-t/\tau}$, the so-called weak kernel, which is frequently used in the literature. Then, the characteristic equation reduces to

$$\tau\lambda^2 + (1 + \alpha d\tau)\lambda + \alpha(s+d) = 0. \tag{B.9}$$

It is easy to verify that the two eigenvalues of (B.9) have negative real parts and hence that system (B.6) in this case is always locally stable.

Appendix C. Model extension: nonlinear demand and supply curves

Nonlinear demand and supply curves have been found to generate complex price dynamics and chaotic behavior in discrete-time cobweb models (Goeree and Hommes, 2000 and Chiarella et al., 2006). This section investigates the global dynamics with nonlinear supply curves and linear demand. To analytically derive the corresponding cost function, we assume an *S*-shaped supply curve

$$S(H) = \operatorname{arsinh}(sH), \tag{C.1}$$

but other choices for the *S*-shaped supplies yield similar results (Hommes, 1994). Equation (C.1) implies a cost function of

$$c(q) = \frac{1}{s}[\cosh(q) - 1]. \tag{C.2}$$

Thus, the realized net profits are given by

$$\begin{aligned} \pi_t^R &= P_t S(P_t) - c(S(P_t)) - C = P_t \operatorname{arsinh}(sP_t) - \sqrt{1/s^2 + P_t^2} + 1/s - C, \\ \pi_t^N &= P_t S(P_{t-\tau}) - c(S(P_{t-\tau})) = P_t \operatorname{arsinh}(sP_{t-\tau}) - \sqrt{1/s^2 + P_{t-\tau}^2} + 1/s, \end{aligned} \tag{C.3}$$

and the complete cobweb-type model with nonlinear supply is given by

$$\begin{cases} \dot{P}_t = \alpha\Big[A - dP_t - n_{t-\tau}^R \operatorname{arsinh}(sP_t) - (1 - n_{t-\tau}^R)\operatorname{arsinh}(sP_{t-\tau})\Big], \\ \dot{U}_t^R = \eta\Big[P_t \operatorname{arsinh}(sP_t) - \sqrt{1/s^2 + P_t^2} + 1/s - C - U_t^R\Big], \\ \dot{U}_t^N = \eta\Big[P_t \operatorname{arsinh}(sP_{t-\tau}) - \sqrt{1/s^2 + P_{t-\tau}^2} + 1/s - U_t^N\Big]. \end{cases} \tag{C.4}$$

Intuitively, given the monotonically increasing supply curves $\operatorname{arsinh}(\cdot)$, there should be a unique positive steady-state price, while the *S*-shaped supply curves should enlarge the steady-state price. It follows from the first equation of (C.4) that the steady-state price is governed by $\operatorname{arsinh}(sP^*) = A - dP^*$ and $0 < P^* < A/d$. Hence, the nonlinear supply does shift the steady-state price and the realized profits, while the market fraction in the steady state $n^{R*} = \tanh(-\beta C/2)$ is still the same as that in system (3.6) with linear supply curves. The local dynamics of system (C.4) are given by the following proposition.

Proposition C.1.

(1) *System (C.4) has a unique steady state* (P^*, U^{R*}, U^{N*}).
(2) *If* $s \le d\sqrt{1 + s^2(P^*)^2}/(1 - 2n^{R*})$, *then* (P^*, U^{R*}, U^{N*}) *is locally asymptotically stable for all* $\tau \ge 0$.
(3) *If* $s > d\sqrt{1 + s^2(P^*)^2}/(1 - 2n^{R*})$, *then* (P^*, U^{R*}, U^{N*}) *is locally asymptotically stable for* $0 < \tau < \tilde{\tau}_0^*$, *is unstable for* $\tau > \tilde{\tau}_0^*$, *and undergoes a Hopf bifurcation at* $\tau = \tilde{\tau}_0^*$, *where* $\tilde{\tau}_0^*$ *is governed by (C.5).*

Proof. There is a unique steady state (P^*, U^{R*}, U^{N*}) of system (C.4) where P^* is governed by $\operatorname{arsinh}(sP^*) = A - dP^*$ and

$$\begin{aligned} U^{R*} &= P^* \operatorname{arsinh}(sP^*) - \sqrt{\tfrac{1}{s^2} + (P^*)^2} + \tfrac{1}{s} - C, \\ U^{N*} &= P^* \operatorname{arsinh}(sP^*) - \sqrt{\tfrac{1}{s^2} + (P^*)^2} + \tfrac{1}{s}. \end{aligned}$$

The characteristic equation of system (C.4) in the steady state (P^*, U^{R*}, U^{N*}) is given by

$$(\lambda + \eta)^2 \left\{ \lambda + \alpha\left[d + \frac{sn^{R*}}{\sqrt{1 + s^2(P^*)^2}} \right] + \frac{\alpha s(1 - n^{R*})}{\sqrt{1 + s^2(P^*)^2}} e^{-\lambda\tau} \right\} = 0,$$

where $n^{R*} = \tanh(-\beta C/2)$. Following the same analysis of Appendices A.2-A.3, we obtain Proposition Appendix C.1, where $\tilde{\tau}_n^*$ is given by

$$\tilde{\tau}_n^* = \frac{1}{\tilde{\omega}^*}\left[\cos^{-1}\left(-\frac{d\sqrt{1 + s^2(P^*)^2} + sn^{R*}}{s(1 - n^{R*})} \right) + 2n\pi \right], \quad n = 0, 1, 2, \cdots, \tag{C.5}$$

and

$$\tilde{\omega}^* = \alpha \sqrt{\frac{s^2(1 - n^{R*})^2}{1 + s^2(P^*)^2} - \left[d + \frac{sn^{R*}}{\sqrt{1 + s^2(P^*)^2}} \right]^2}.$$

□

The *S*-shaped supply curves limit the destabilizing effect of naive predictors and hence stabilize system (C.4) with nonlinear supply by enlarging the corresponding stability ranges in the linear-supply case (3.6) in the sense that $d\sqrt{1 + s^2(P^*)^2}/(1 - 2n^{R*}) > d/(1 - 2n^{R*})$ and $\tilde{\tau}_0^* > \tau_0^*$.

Despite the different supply curves, Proposition Appendix C.1 shares the same message as Proposition 3.3 on local stability with respect to the role of the intensity of choice and perfect-foresight and naive expectations (except for a shift in the

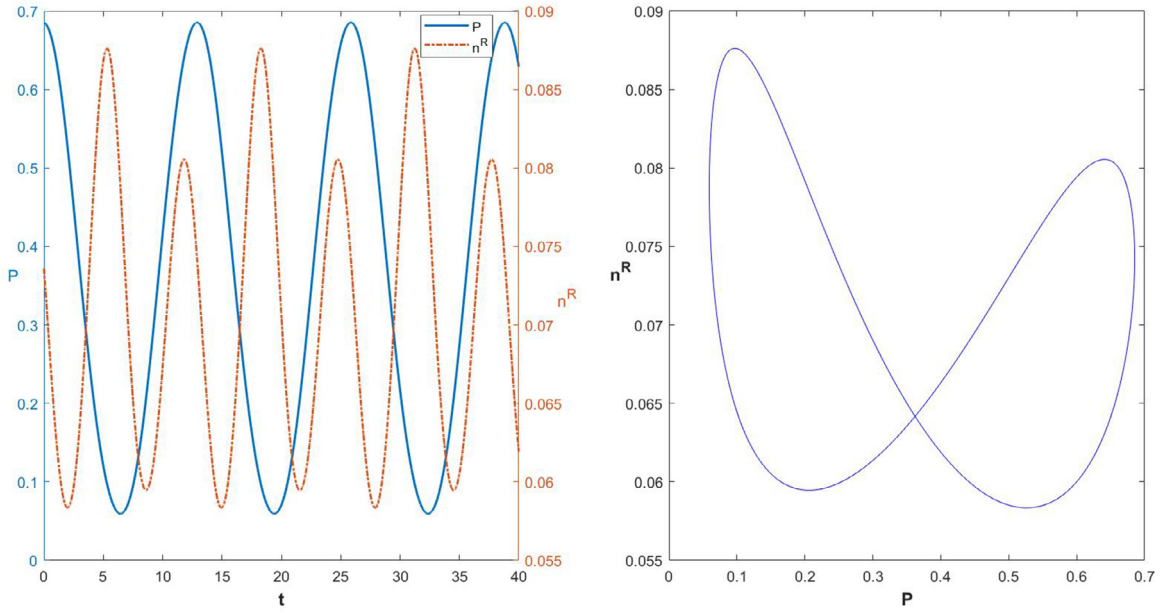

Fig. C1. The left panel illustrates the price time series and market fraction of perfect-foresight traders, and the right panel illustrates the phase plot. Here, $\tau = 5$, $\beta = 3$, $\alpha = 0.5$, $A = 1$, $d = 1$, $s = 2$, $\eta = 0.5$, and $C = 1$.

steady state). In fact, all the analyses in Propositions 3.1–3.6 can be extended to the nonlinear demand and supply cases. The local stability is still the same, except that the bifurcation values and steady states may be changed, and the dynamics become more involved.

Figure C.1 illustrates the dynamics of (C.4) with nonlinear supply. Under this set of parameters, the steady state is $(P^*, U^{R*}, U^{N*}) = (0.35, -0.88, 0.12)$, and the market fraction of perfect-foresight traders in the steady state is $n^{R*} = 0.05$. Numerical simulations (not reported here) show that the price bifurcations with respect to τ and β are similar to those in Fig. 3.1. Interestingly, the right panel shows that the price and fraction converge to a *figure-eight-shaped* attractor, a phenomenon also observed in He and Li (2012). During one price cycle, the market fraction fluctuates up and down twice. The market prices are close to the steady-state price ($P^* = 0.35$) whenever the market fractions of naive traders are high.

Brock and Hommes (1997) and Goeree and Hommes (2000) show that nonlinear cobweb models with population evolutions exhibit complex behavior of coexistence of attractors. However, we do not find this coexistence for our continuous-time models via numerical simulations even with nonlinear supply. With both nonlinear demand and supply curves, the system may generate richer global dynamics, such as the coexistence of attractors. We leave these investigations to future research.

Appendix D. The long-memory limit

System (3.6) can be simplified by introducing new variables

$$p_t = P_t/A, \quad u_t = \beta U_t^R - \beta U_t^N, \quad \gamma = \frac{\beta s A^2}{2}, \quad C = \beta C_R, \quad n_t = n_t^R.$$

Additionally, after setting the time scale appropriately, we can assume that $\alpha = 1$. The model then takes the simpler form

$$\begin{cases} \dot{p}_t = 1 - d p_t - s n_{t-\tau} p_t - s(1 - n_{t-\tau}) p_{t-\tau}, \\ \dot{u}_t = \eta \Big[\gamma (p_t - p_{t-\tau})^2 - C - u_t \Big]. \end{cases} \tag{D.1}$$

System (D.1) has a unique steady state $(p^*, u^*) = (\frac{1}{d+s}, C)$. This motivates a final variable change

$$p_t = p^* + x_t,$$

which results in the system

$$\dot{x}_t = -d x_t - s n_{t-1} x_t - s(1 - n_{t-1}) x_{t-1}, \tag{D.2}$$

$$\dot{u}_t = \eta \Big[\gamma (x_t - x_{t-1})^2 - C - u_t \Big], \tag{D.3}$$

where without loss of generality we use $\tau = 1$ by setting the time scale.

We introduce new variables R_t and ϕ_t by setting $x_t = \mathrm{Re}\, R_t e^{i\phi_t}$, by which the system (D.2)–(D.3) is transformed to

$$\dot{R}_t = -(d + sn_{t-1})R_t - s(1 - n_{t-1})R_{t-1}\cos(\phi_t - \phi_{t-1}), \tag{D.4}$$

$$\dot{\phi}_t = -s(1 - n_{t-1})\frac{R_{t-1}}{R_t}\sin(\phi_t - \phi_{t-1}), \tag{D.5}$$

$$\dot{u}_t = \eta\Big[\gamma(R_t\cos\phi_t - R_{t-1}\cos\phi_{t-1})^2 - C - u_t\Big]. \tag{D.6}$$

If $\eta \to 0$, the fitness measures U_t^i have a tendency to weight all past profits from a strategy equally; hence, we call this case the long-memory limit. In this limit, system (3.6) can be cast in the mold of a fast–slow system, with the price dynamics of the fast subsystem and the performance difference u_t of the slow subsystem.[17] If $\eta = 0$, the performance difference and hence the fractions n_{t-1} reduce to constants n in the fast subsystem. It can be shown that (R_t, ϕ_t) then converges to an expression of the form $(re^{\mu t}, \varphi + \omega t)$, where (μ, ω) satisfies

$$\mu = -(d + sn) - s(1 - n)e^{-\mu}\cos(-\omega), \tag{D.7}$$

$$\omega = -s(1 - n)e^{-\mu}\sin(-\omega). \tag{D.8}$$

Of course, $\mu + i\omega$ is the eigenvalue of the linearized delay system. Replacing n with $n(u)$, let $(\bar{\mu}(u), \bar{\omega}(u))$ be that solution of (D.7)–(D.8) for which the value of μ is largest, and set $\mu_t = \bar{\mu}(u_t)$, $\omega_t = \bar{\omega}(u_t)$. Note that these are slow-moving variables, with $\dot{\mu}_t = O(\eta)$, etc. However, then $r_t := R_t e^{-\mu_t t}$ and $\varphi_t = \phi_t - \omega_t t$ are slow-moving as well, and, neglecting $O(\eta)$ terms, we obtain the following three-dimensional approximative dynamical system:

$$\dot{\phi}_t = \omega_t, \tag{D.9}$$

$$\dot{R}_t = \mu_t R_t, \tag{D.10}$$

$$\dot{u}_t/\eta = \gamma R_t^2\Big[\cos\phi_t - e^{-\mu_t}\cos(\phi_t - \omega_t)\Big]^2 - 1 - u_t. \tag{D.11}$$

This is a system on the phase space $\mathbb{T} \times \mathbb{R}^2$, for which the set $\mathbb{T} \times \{R = 0\} \times \mathbb{R}$ is invariant. On this set, there is the relative equilibrium $\mathbb{T} \times \{(R, u) = (0, -1)\}$, which corresponds to the fundamental equilibrium $x_t = 0$, $u_t = -1$. As the eigenvalues are $-\eta$ and $\bar{\mu}(-1)$, the stability of the equilibrium is controlled by the latter eigenvalue. It changes the stability if $\bar{\mu} = 0$. From equation (D.7), we obtain first

$$\cos\omega = -\frac{d + sn}{s(1 - n)}.$$

Equation (D.8) then yields

$$\omega = s(1 - n)\sqrt{1 - \cos^2\omega} = \sqrt{s^2(1 - n)^2 - (d + sn)}. \tag{D.12}$$

Using $\cos^2(-\omega) + \sin^2(-\omega) = 1$, with the values of the cosine and the sine solved from equations (D.7) and (D.8),

$$s^2(1 - n)^2 = (d + sn)^2 + \omega^2.$$

Substituting (D.12), this reduces to

$$(d + sn)(d + sn - 1) = 0.$$

As $d > 0$, this equation obtains only if

$$n = \frac{1 - d}{s} \quad \text{or} \quad \frac{1 - d}{s} = \frac{1}{1 + e^{\beta}}.$$

Recall that at $u = -1$, we have $n = 1/(1 + e^{\beta})$. Hence a Hopf bifurcation can take place only if $0 \le n \le \frac{1}{2}$, the extreme values corresponding to $C = \infty$ and $C = 0$, respectively.

[17] If $\eta \to \infty$, the fitness measures U_t^i are driven by the most recent profits; hence, we call this case the short-memory limit. In this limit, system (3.6) can also be cast in the mold of a fast–slow system, with price dynamics now being the slow subsystem and the performance difference u_t the fast subsystem.

References

Anderson, S., de Palma, A., Thisse, J., 1992. Discrete Choice Theory of Product Differentiation. MIT Press, Cambridge, MA.
Asada, T., Yoshida, H., 2001. Stability, instability and complex behavior in macrodynamic models with policy lag. Discrete Dyn. Nat. Soc. 5, 281–295.
Beja, A., Goldman, M., 1980. On the dynamic behavior of prices in disequilibrium. J. Finance 35, 235–247.
Branch, W., 2002. Local convergence properties of a cobweb model with rationally heterogeneous expectations. J. Econ. Dyn. Control 27, 63–85.
Brock, W., Hommes, C., 1997. A rational route to randomness. Econometrica 65, 1059–1095.
Brock, W., Hommes, C., 1998. Heterogeneous beliefs and routes to chaos in a simple asset pricing model. J. Econ. Dyn. Control 22, 1235–1274.
Brock, W., Hommes, C., Wagener, F., 2005. Evolutionary dynamics in financial markets with many trader types. J. Math. Econ. 41, 7–42.
Chiarella, C., 1988. The cobweb model: its instability and the onset of chaos. Econ. Model. 5, 377–384.
Chiarella, C., He, X., 2003. Dynamics of beliefs and learning under a_l-processes – the heterogeneous case. J. Econ. Dyn. Control 27, 503–531.
Chiarella, C., He, X., Hung, H., Zhu, P., 2006. An analysis of the cobweb model with boundedly rational heterogeneous producers. J. Econ. Behav. Organ. 61, 750–768.
Day, R., Huang, W., 1990. Bulls, bears and market sheep. J. Econ. Behav. Organ. 14, 299–329.
Di Guilmi, C., He, X., Li, K., 2014. Herding, trend chasing, and market volatility. J. Econ. Dyn. Control 48, 349–373.
Dieci, R., Westerhoff, F., 2010. Interacting cobweb markets. J. Econ. Behav. Organ. 75, 461–481.
Diks, C., van der Weide, R., 2005. Herding, a-synchronous updating and heterogeneity in memory in a CBS. J. Econ. Dyn. Control 29, 741–763.
Ezekiel, M., 1938. The cobweb theorem. Q. J. Econ. 52, 255–280.
Franke, R., Asada, T., 2008. Incorporating positions into asset pricing models with order-based strategies. J. Econ. Interact. Coord. 3, 201–227.
Goeree, J., Hommes, C., 2000. Heterogeneous beliefs and the non-linear cobweb model. J. Econ. Dyn. Control 24, 761–798.
Gori, L., Guerrini, L., Sodini, M., 2014. Hopf bifurcation in a cobweb model with discrete time delays. Discrete Dyn. Nat. Soc. 137090.
Gori, L., Guerrini, L., Sodini, M., 2015. Equilibrium and disequilibrium dynamics in cobweb models with time delays. Int. J. Bifurcation Chaos 25, 1550088.
Guo, B., Huang, F., Li, K., 2020. Time to build and bond risk premia. J. Econ. Dyn. Control 121, 104024.
Haldane, J., 1932. A contribution to the theory of price fluctuations. Rev. Econ. Stud. 1, 186–195.
He, X., Li, K., 2012. Heterogeneous beliefs and adaptive behaviour in a continuous-time asset price model. J. Econ. Dyn. Control 36, 973–987.
He, X., Li, K., 2015. Profitability of time series momentum. J. Bank. Finance 53, 140–157.
He, X., Li, K., Wei, J., Zheng, M., 2009. Market stability switches in a continuous-time financial market with heterogeneous beliefs. Econ. Model. 26, 1432–1442.
Hofbauer, J., Sigmund, K., 1998. Evolutionary Games and Population Dynamics. Cambridge University Press.
Hommes, C., 1994. Dynamics of the cobweb model with adaptive expectations and nonlinear supply and demand. J. Econ. Behav. Organ. 24, 315–335.
Hommes, C., 1998. On the consistency of backward-looking expectations: the case of the cobweb. J. Econ. Behav. Organ. 33, 333–362.
Hommes, C., 2011. The heterogeneous expectations hypothesis: some evidence from the lab. J. Econ. Dyn. Control 35, 1–24.
Hommes, C., 2018. Carl's nonlinear cobweb. J. Econ. Dyn. Control 91, 7–20.
Hommes, C., Sonnemans, J., Tuinstra, J., van de Velden, H., 2007. Learning in cobweb experiments. Macroecon. Dyn. 11, 8–33.
Hommes, C., Wagener, F., 2010. Does eductive stability imply evolutionary stability? J. Econ. Behav. Organ. 75, 25–39.
Jensen, R., Urban, R., 1984. Chaotic price behaviour in a non-linear cobweb model. Econ. Lett. 15, 235–240.
Kydland, F., Prescott, E., 1982. Time to build and aggregate fluctuations. Econometrica 50, 1345–1370.
Lani-Wayda, B., Walther, H., 1995. Chaotic motion generated by delayed negative feedback. Part I: a transversality criterion. Differ. Integral Equ. 8, 1407–1452.
Lani-Wayda, B., Walther, H., 1996. Chaotic motion generated by delayed negative feedback. Part II: construction of nonlinearities. Mathematische Nachrichten 180, 141–211.
Li, K., 2019. Portfolio selection with inflation-linked bonds and indexation lags. J. Econ. Dyn. Control 107, 103727.
Li, K., Liu, J., 2018. Portfolio Selection under Time Delays: A Piecewise Dynamic Programming Approach. working paper. Available at SSRN: https://ssrn.com/abstract=2916481
Li, K., Liu, J., 2021. Optimal dynamic momentum strategies. Oper. Res.. Forthcoming
Li, K., Wei, J., 2009. Stability and Hopf bifurcation analysis of a prey-predator system with two delays. Chaos Solitons Fractals 42, 2606–2613.
MacDonald, N., 1978. Time lags in biological systems. Lecture Notes in Biomathematics, Vol. 27. Springer, London.
Mackey, M., 1989. Commodity price fluctuations: price dependent delays and nonlinearities as explanatory factors. J. Econ. Theory 48, 497–509.
Matsumoto, A., Nakajama, K., 2015. Nonlinear cobweb model with time delays. In: International Conference on Modeling, Simulation and Applied Mathematics, pp. 402–406.
Matsumoto, A., Szidarovszky, F., 2015. The asymptotic behavior on a nonlinear cobweb model with time delays. Discrete Dyn. Nat. Soc. 312574.
Mitra, S., Boussard, J.M., 2012. A simple model of endogenous agricultural commodity price fluctuations with storage. Agric. Econ. 43, 1–15.
Onozaki, T., Sieg, G., Yokoo, M., 2003. Stability, chaos and multiple attractors: a single agent makes a difference. J. Econ. Dyn. Control 27, 1917–1938.
Ott, E., 1993. Chaos in Dynamical Systems. Cambridge University Press, New York.
Phillips, A., 1957. Stabilisation policy and the time-forms of lagged responses. Econ. J. 67, 265–277.
Schmitt, N., Westerhoff, F., 2015. Managing rational routes to randomness. J. Econ. Behav. Organ. 116, 157–173.
Sonnemans, J., Hommes, C., Tuinstra, J., van de Velden, H., 2004. The instability of a heterogeneous cobweb economy: a strategy experiment on expectation formation. J. Econ. Behav. Organ. 54, 453–481.
Steinlein, H., Walther, H., 1990. Hyperbolic sets, transversal homoclinic trajectories, and symbolic dynamics for C^1-maps in Banach spaces. J. Dyn. Differ. Equ. 2, 325–365.
Yoshida, H., Asada, T., 2007. Dynamic analysis of policy lag in a Keynes-Goodwin model: stability, instability, cycles and chaos. J. Econ. Behav. Organ. 62, 441–469.
Zhu, M., Chiarella, C., He, X., Wang, D., 2009. Does the market maker stabilize the market? Physica A 388, 3164–3180.
Zuo, W., Song, Y., 2015. Stability and bifurcation analysis of a reaction-diffusion equation with spatio-temporal delay. J. Math. Anal. Appl. 430, 243–261.